

Human Immunodeficiency Virus-Induced Apoptosis of Human Breast Cancer Cells *Via* CXCR4 is Mediated by the Viral Envelope Protein But Does Not Require CD4

Masafumi Endo, Asako Inatsu, Koji Hashimoto, Nobutoki Takamune, Shozo Shoji and Shogo Misumi*

Department of Pharmaceutical Biochemistry, Faculty of Medical and Pharmaceutical Science, Kumamoto University, Kumamoto, Japan

Abstract: HIV-1 infection results in an increased risk of malignancy as well as immune suppression. However, analyses of cancer incidence in chronically immunosuppressed transplant recipients and HIV-infected person have demonstrated an unexpected low incidence of certain types of cancer, such as breast cancers, and the mechanism behind this remains unclarified. In this study, we show that most breast cancer cell lines express CXCR4 but are not susceptible to HIV-1 infection. The apoptosis of breast cancer cells is induced by HIV-1 in a viral-dose- and time-dependent manner without productive infection. The apoptosis is induced by R5X4 and X4 HIV-1 but not by R5 HIV-1, and is inhibited by an anti-CXCR4 antibody, an anti-gp120 antibody, AMD3100, or pertussis toxin. The apoptosis is mediated *via* CXCR4 in breast cancer cells that exhibit conformational heterogeneity in comparison with CXCR4 in T-cells. Furthermore, the gp120 mutant (E370R) with a low CD4 binding ability can specifically induce apoptosis in breast cancer cells but not in T-cells. Taken together, these results indicate that HIV-1 and gp120 can induce breast cancer cell apoptosis through gp120-CXCR4 interaction without a CD4-induced conformational change of gp120, and may lead to a novel HIV-1-based therapy for breast cancer.

Keywords: Breast cancer, HIV-1 envelope protein, apoptosis, CXCR4.

Human immunodeficiency virus type 1 (HIV-1) infection is associated with the depletion of CD4⁺ T-cells. The phenomenon renders the host susceptible to opportunistic infections through the dysregulation and dysfunction of the immune system [1, 2]. HIV-1 infection also results in an increased susceptibility to malignant tumors caused by a decreased immunologic response to tumor cells and an increased susceptibility to oncogenic viral infection [3, 4]. Indeed, people infected with HIV are at a high risk of developing cancer [5-7]. Cancers in HIV-1-infected patients can be divided into three groups. The first group includes AIDS-defining cancers such as Kaposi's sarcoma [7]. The second group includes malignancies more prevalent among patients with HIV infection such as Hodgkin's lymphoma, squamous cell carcinoma of the anus, and lung cancer [5, 8-10]. The third group includes cancers whose incidences are not increased by HIV infection such as breast cancer [10-12]. Several hypotheses explaining the low incidence of breast cancer among HIV-1-infected patients have been proposed (e.g., immunodeficiency, socioeconomic state, racial disparity, metabolic complications of antiretroviral therapy, and a short life span of HIV-1-infected patient) [10-15].

HIV-1 uses CD4 and a chemokine receptor for cellular entry [16]. After the binding of the HIV-1 envelope glycoprotein (Env) gp120 to CD4, gp120 changes its conformation to bind to the chemokine receptor and initiates fusion

with the cellular membrane. The chemokine receptors CCR5 and CXCR4 are the main coreceptors for the cellular entry of HIV-1. In general, viral strains are classified into R5, X4 and R5X4 according to the usage of chemokine receptor [17]. The HIV-1 R5 virus is generally transmitted and predominates at the early stage of HIV-1 infection. In contrast, R5X4 and X4 viruses emerge at the later stage of infection, and their emergence is frequently associated with a rapid depletion of CD4⁺ T-cells [18, 19].

Besides the viral entry, the binding of virion-associated gp120 to coreceptors induces physiological effects that are relevant to pathogenesis. In particular, the binding of gp120 to CCR5 [20-22] or CXCR4 [22, 23] was shown to trigger the apoptosis of both infected and uninfected T-cells, which represents a fundamental mechanism of immunodeficiency syndrome. HIV-1 isolates differ in their ability to induce the apoptosis of bystander uninfected cells and infected cells themselves, and apoptosis determinants seem to be located in gp120 [24, 25]. Although the precise regions in gp120 that can induce apoptosis have not been identified yet, HIV-1 gp120, which interacts with CXCR4, seems to have highly cytopathic effects because CXCR4 is expressed in a wide range of target cells [26-28].

CXCR4 has recently been shown to be expressed on primary tumours of human invasive lobular or ductal breast carcinoma and to mediate organ-specific metastasis [29, 30]. Therefore, we investigated the biological effect of HIV-1 on breast cancer cells. In this study, we observed the HIV-1-induced apoptosis of breast cancer cells without productive infection. Furthermore, the induction of apoptosis was critically dependent on the interaction of gp120 with CXCR4 without a CD4-induced conformational change of gp120.

*Address correspondence to this author at the Department of Pharmaceutical Biochemistry, Faculty of Medical and Pharmaceutical Science, Kumamoto University, 5-1 Oe-Honmachi, Kumamoto 862-0973, Japan; Tel: +81-96-371-4362; Fax: +81-96-362-7800; E-mail: misumi@gpo.kumamoto-u.ac.jp

The gp120 mutant E370R specifically induces the apoptosis of breast cancer cells but not T-cells. These results indicate the possibility of developing a novel HIV-1-based breast cancer therapy.

MATERIAL AND METHODS

Cell Culture and HIV-1 Preparations

Human T lymphoblastoid cell lines (CEM, CEM-CCR5 and Molt4#8), a chronically HIV-1-infected T-cell line (CEM/LAV-1), and human breast cancer cell lines (MCF-7, and DU4475) were maintained at 37°C in the RPMI-1640 medium supplemented with 10% fetal calf serum (FCS) containing 100 IU/ml penicillin and 100 µg/ml streptomycin in 5% CO₂. The human breast cancer cell lines (MDA-MB-453 and MDA-MB-231) were maintained at 37°C in Dulbecco's modified Eagle's medium (DMEM) supplemented with 10% FCS containing 100 IU/ml penicillin and 100 µg/ml streptomycin in 5% CO₂.

For the preparation of infectious HIV-1, supernatants of the culture media of acutely HIV-1-infected cells (CEM-CCR5 for the JRFL strain, and CEMx174 for the 89.6 strain) and chronically HIV-1-infected T-cells (CEM/LAV-1 for the LAV-1 strain) were separately filtered through 0.45-µm-pore-size filters. The viral preparation was stored at -80°C until use.

Flow Cytometry

To compare the expression level of CD4 or CXCR4, cells (1×10^5) were washed with washing buffer (PBS containing 2% FCS and 0.02% NaN₃) and incubated with 10 µg/ml primary antibody (Leu-3a (Becton Dickinson Immunocytometry System), 12G5 (R & D Systems), 44717.111 (R & D Systems), IA2F9 [31], or the anti-CXCR4 N-terminal rabbit polyclonal antibody (Affinity BioReagents, Inc.) for 30 min at 4°C. The cells were then washed with the same washing buffer and incubated with suitable FITC-labeled secondary antibodies. The cells were washed again, and analyzed using an EPICS XL flow cytometer (Beckman Coulter).

Determination of Chemokine Receptor by SYBR Green Real-Time PCR Analysis

To determine CXCR4 expression in the breast cancer cell lines, total RNA of each cell line was extracted by the acid guanidinium phenol chloroform method using an ISOGEN kit (Nippon Gene). The extracted total RNA was reverse-transcribed to cDNA using Moloney-Murine Leukemia Virus Reverse Transcriptase and the Oligo-dT primer (Parkin Elmer, Roche Molecular Systems, Inc.). SYBR green real-time PCR analysis was performed using a DNA Engine Opticon 2 fluorescence detection system (MJ Research) and a DyNAmo HS SYBR green qPCR kit (MJ Research) according to the manufacturer's instructions. The primer pair of *human CCR5* (5'-GGACCAAGCTATGCAGGTGAC-3' and 5'-TTGGCACTGTGCTTTTGGAA-3') was used. PCR amplification was carried out using the following cycles: one cycle of 15 min at 95°C and 40 cycles in four steps for each (95°C for 10s, 57°C for 20s, 72°C for 20s, and 76°C for 2s). At the end of the cycles, melting temperature analysis was performed by gradually increasing temperature (0.5°C/s) to 95°C.

Detection of p24 Antigen and Total Viral DNA

To investigate whether breast cancer cells are actually resistant to HIV-1 infection, CEM cells (1×10^5), DU4475 and MCF7 cells (1×10^5) were inoculated with HIV-1_{LAV-1} or HIV-1_{89.6} (100 ng of the HIV-1 p24 antigen) and incubated at 37°C for 2h. The cells were washed twice and cultured at 37°C for 10 days. Then the culture supernatant of each cell line was collected, and p24 antigen level was measured by antigen-capture enzyme-linked assay using a RETRO-TEK HIV-1 p24 antigen enzyme-linked immunosorbent assay kit (ZeptoMatrix Corp.) according to the manufacturer's instructions. For the detection of total viral DNA, total DNA obtained after the purification procedure was subjected to SYBR green real-time PCR analysis as described above. The following primer pair was used: HIV-1 *pol* (5'-TACAGGAGCAGATGATACAG-3' and 5'-CCTG GCTTAATTTACTGG-3').

Annexin-V Staining Assay

To detect the annexin V-positive cells, an Annexin V-FLUOS staining kit (Roche Diagnostics GmbH) was used according to the manufacturer's recommendation. DU4475 and MCF-7 cells (1×10^6) were plated in 24-well plates and preincubated with or without increasing concentrations of pertussis toxin (SIGMA). This was followed by treatment with HIV-1 (100 ng of the HIV-1 p24 antigen) and incubation in 1 ml of a fresh medium at 37°C for 36h. Then the cells were harvested and resuspended in 100 µl of staining solution (containing annexin V-fluorescein and propidium iodide), and were mixed gently and incubated for 15 min at room temperature (15-25°C) in the dark. The samples were analyzed in an EPICS XL flow cytometer (Beckman Coulter).

Coculture Assay

Cocultivation of MCF-7 cells was carried out in a transwell to show whether gp120 induced apoptosis *via* CXCR4. HEK293 cells were transfected with a vector-derived mRNA (control), or an mRNA encoding HIV-1_{89.6} gp120 WT or gp120 mutant (E370R). In the lower chamber, MCF-7 (1×10^6) or CEM (1×10^6) cells were incubated with HEK293 cells, which were placed in the upper chamber of a 3-µm-pore-size transwell (Corning, NY). After 48h of coculture, MCF-7 or CEM cells were subjected to Annexin-V staining assay.

TUNEL Assay

To detect the TUNEL-positive cells, DU4475 and MCF-7 cells (1×10^6) were washed with phosphate-buffered saline (PBS), and then preincubated with or without 20 µl of an anti-CD4 antibody (Leu-3a; Becton Dickinson Immunocytometry System), 5 µg of an anti-CXCR4 antibody (12G5; R & D Systems), or 2 µM AMD3100 (NIH AIDS Research and Reference Reagent Program) on ice for 30 min. The cells were then inoculated with HIV-1 (100 ng) preincubated with or without 5 µg of a cross-reactive anti-gp120 antibody (ImmunoDiagnostica), and cultured in 5 ml of a fresh medium at 37°C for 36h. Then the cells were harvested and subjected to an assay using a DeadEnd Fluorometric TUNEL system (Promega Corporation) according to the manufacturer's instructions.

RESULTS

Profiles of CXCR4 and CD4 Expressions on Breast Cancer Cells

The expression of either CCR5 or CXCR4 is one of the indicators of the susceptibility of CD4⁺ target cells to HIV-1 infection [16]. Flow cytometry showed that CXCR4 was expressed on breast cancer cell lines (Fig. 1A) and CD4 was expressed at a high level on Molt4#8 cells, but not on DU4475 and MCF-7 cells (Fig. 1B). Furthermore, the RNA expression levels of CCR5 determined by quantitative real-time PCR analysis showed that most of the breast cancer cell lines have low or undetectable levels of CCR5 expression (data not shown).

Breast Cancer Cells are Resistant to HIV-1 Infection

Because CD4 is the primary receptor for the cellular entry of HIV-1, the absence of CD4 expression on breast cancer cells implies that they are resistant to HIV-1 infection. To investigate whether breast cancer cells are actually resistant to HIV-1 infection, conventional infection assays measuring HIV-1 proviral DNA and the HIV-1 p24 antigen were performed. DU4475 and MCF-7 cells were inoculated with HIV-1_{LAV-1}, which utilizes CXCR4 and CD4 for cellular entry, and incubated for 10 days. In human T lymphoblastoid CEM cells, HIV-1 total DNA was detected (Fig. 1C) and abundant progeny virus was produced (Fig. 1D). On the other hand, the total viral DNA level in breast cancer cells was less than 1/1000 that in CEM cells (Fig. 1C) and the p24

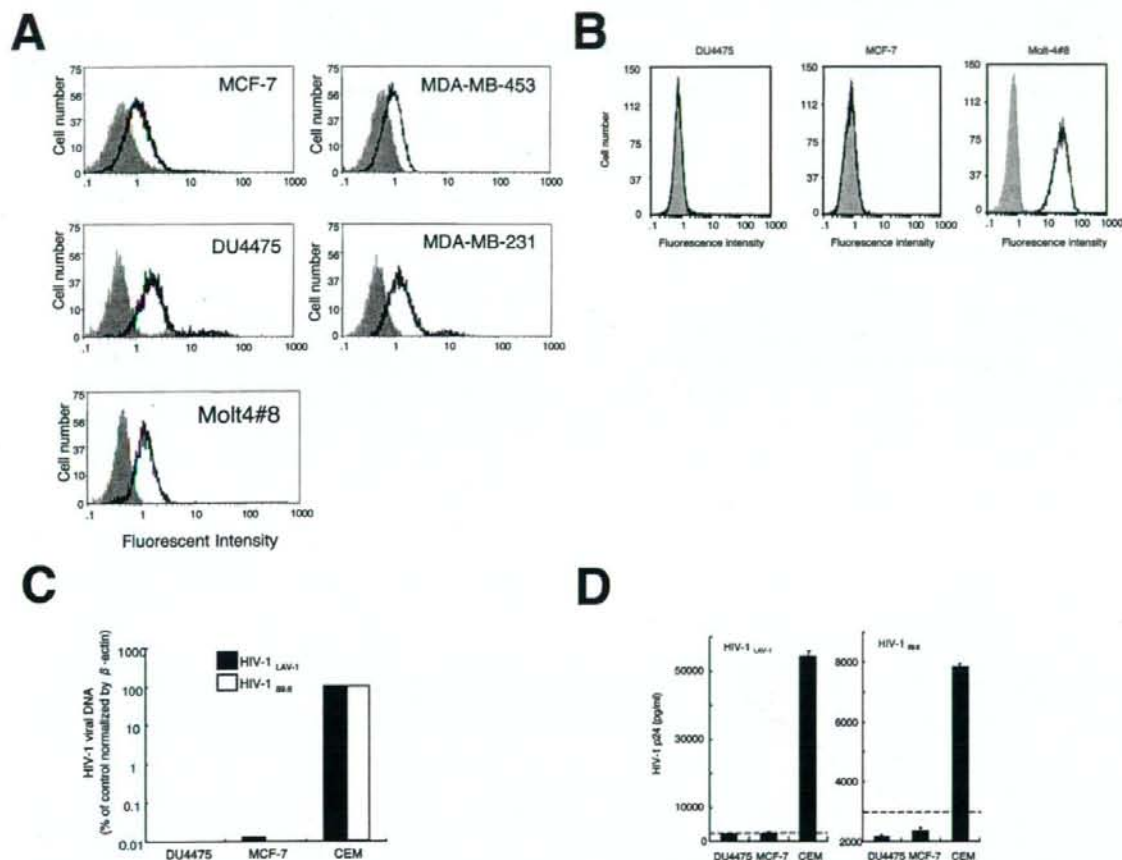


Fig. (1). Breast cancer cells are resistant to HIV-1 infection. (A) Human T-cell line (Molt4#8) and breast cancer cell lines (MCF-7, DU4475, MDA-MB-231 and MDA-MB-453) were incubated with 10 μ g/ml anti-CXCR4 N-terminal (bold line) or isotype control (gray area). Subsequently, cells were incubated with suitable FITC-labeled secondary antibodies, and subjected to flow cytometry. (B) DU4475 and MCF-7 cells, and Molt4#8 cells were incubated with the anti-CD4 antibody (bold line) or the isotype control (gray area) for 30 min at 4°C. Subsequently, the cells were incubated with FITC-conjugated anti-mouse IgG and subjected to flow cytometry. CD4 is expressed at a high level on Molt4#8 cells, but not on DU4475 and MCF-7 cells. (C,D) DU4475 and MCF-7 cells, and CEM cells were inoculated with HIV-1_{LAV-1} or HIV-1_{89.6} (100 ng of the HIV-1 p24 antigen). HIV-1 total DNA (C) and the p24 antigen level of supernatant (D) were measured by quantitative real-time PCR analysis and antigen-capture enzyme-linked assay as described in Materials and Methods. Dotted line in Fig. (1D) indicates the limit of p24 detection in this assay.

antigen level in the culture medium was below the detection limit (Fig. 1D). Similar results were observed in experiments using HIV-1_{89.6} (Fig. 1C,D), suggesting that breast cancer cells are resistant to HIV-1 infection. These results were also consistent with an *in vivo* study [32] that demonstrated that breast cancer cells from HIV-1-infected patients are HIV-1-negative.

HIV-1 Induces Apoptosis of Breast Cancer Cells

In HIV-1-infected patients, many cell types are damaged by bystander apoptosis through several mechanisms and are involved in pathologic processes in these patients [22, 26, 33, 34]. To investigate the HIV-1-induced apoptosis of breast cancer cells, DU4475 cells were inoculated with HIV-1_{89.6} at concentrations ranging from 62.5 to 500 ng of HIV-1 p24, incubated for 36h, and subjected to TUNEL assay to determine the percentage of apoptotic cells. The inoculation of DU4475 cells with increasing doses of HIV-1 showed that HIV-1_{89.6} induced the apoptosis of DU4475 cells in a viral-dose-dependent manner (Fig. 2A). Furthermore, the kinetics of HIV-1-induced apoptosis of DU4475 cells was also investigated. After the inoculation of cells with the virus (250 ng), the cells were subjected to TUNEL assay at different time points (0 to 36h). At incubation times longer than 12h, a significant apoptosis was observed and the percentage of apoptotic cells showed an almost linear relationship with time, suggesting that the HIV-1-induced apoptosis of breast cancer cells occurs in a time-dependent manner (Fig. 2B). At 36h postinoculation, the percentage of apoptotic cells increased more than sevenfold. Taken together, these results indicate that HIV-1 affects the proliferation of breast cancer cells through the induction of their apoptosis.

Induction of Apoptosis of Breast Cancer Cells by HIV-1 is Dependent on Viral Isolate

The cytopathic effect of HIV-1 on bystander cells was diverse among viral strains and was dependent on several

factors including viral coreceptor usage, the affinity between Env and the receptor, and the expression levels of CD4 and chemokine receptors on target cells [22, 24, 28]. To investigate the ability of diverse HIV-1 strains to induce the apoptosis of breast cancer cells, laboratory-adapted (X4 virus, HIV-1_{LAV-1}; R5 virus, HIV-1_{JRFL}; and R5X4 virus, HIV-1_{89.6}) or primary HIV-1 isolates (R5 subtype C virus, HIV-1_{MJ4}; X4 subtype A virus, HIV-1_{92UG029}; and X4 subtype C virus, HIV-1_{98IN017}) were inoculated to DU4475 and MCF-7 cells (Fig. 3). The amount of inoculated virus was normalized to 100 ng of the p24 antigen, and the uninfected-cell supernatant was used as the control. TUNEL assay showed that HIV-1_{LAV-1} (X4) and HIV-1_{89.6} (R5X4) significantly induced the apoptosis of DU4475 and MCF-7 cells (Fig. 3A,B). However, HIV-1_{JRFL} (R5) did not exert any cytopathic effects on both cells (Fig. 3A,B). In agreement with the finding, Annexin-V staining assay showed that the primary isolates HIV-1_{92UG029} (X4A) and HIV-1_{98IN017} (X4C) significantly induced the apoptosis of DU4475 and MCF-7 cells (Fig. 3C,D). However, HIV-1_{MJ4} (R5C) did not exert any cytopathic effects on both cell lines (Fig. 3C,D). These results indicate that the ability of HIV-1 to induce the apoptosis of breast cancer cells was dependent on the viral strain, and it seems that the laboratory-adapted (HIV-1_{LAV-1} and HIV-1_{89.6}) or primary X4 HIV-1 isolates (HIV-1_{92UG029} and HIV-1_{98IN017}) are more potent inducers of apoptosis than the R5 HIV-1 isolates (HIV-1_{JRFL} and HIV-1_{MJ4}).

HIV-1 Induces Breast Cancer Cell Apoptosis Through gp120-CXCR4 Interaction

Because CXCR4 was expressed in DU4475 and MCF-7 cells (Fig. 1), and R5X4 and X4 HIV-1 isolates were more potent inducers of the apoptosis of both cell lines (Fig. 3), we hypothesized that the interaction of viral gp120 with CXCR4 might play critical roles in the induction of the apoptosis of breast cancer cells. To test this hypothesis, DU4475 and MCF-7 cells were preincubated with an anti-

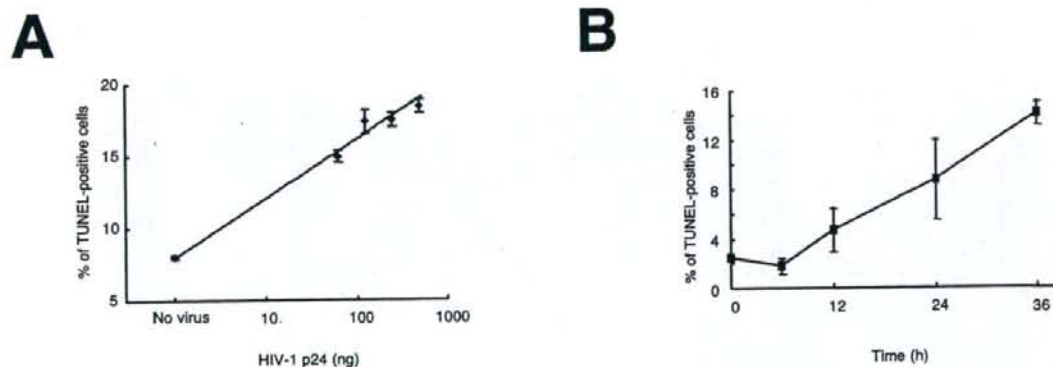


Fig. (2). HIV-1 induces apoptosis of breast cancer cells. To investigate the viral dose kinetics of apoptosis of breast cancer cells, DU4475 cells were inoculated with the culture supernatant of uninfected cells or various amounts of HIV-1_{89.6} (62.5, 125, 250, 500 ng of the HIV-1 p24 antigen). After a 36h incubation, the cells were subjected to TUNEL assay to determine the percentage of apoptotic cells (A). To further investigate the time kinetics of apoptosis of breast cancer cells, DU4475 cells were inoculated with HIV-1_{89.6} (250 ng of HIV-1 p24 antigen) and incubated for 0, 6, 12, 24 and 36h, and subsequently harvested and subjected to TUNEL assay to determine the percentage of apoptotic cells (B).

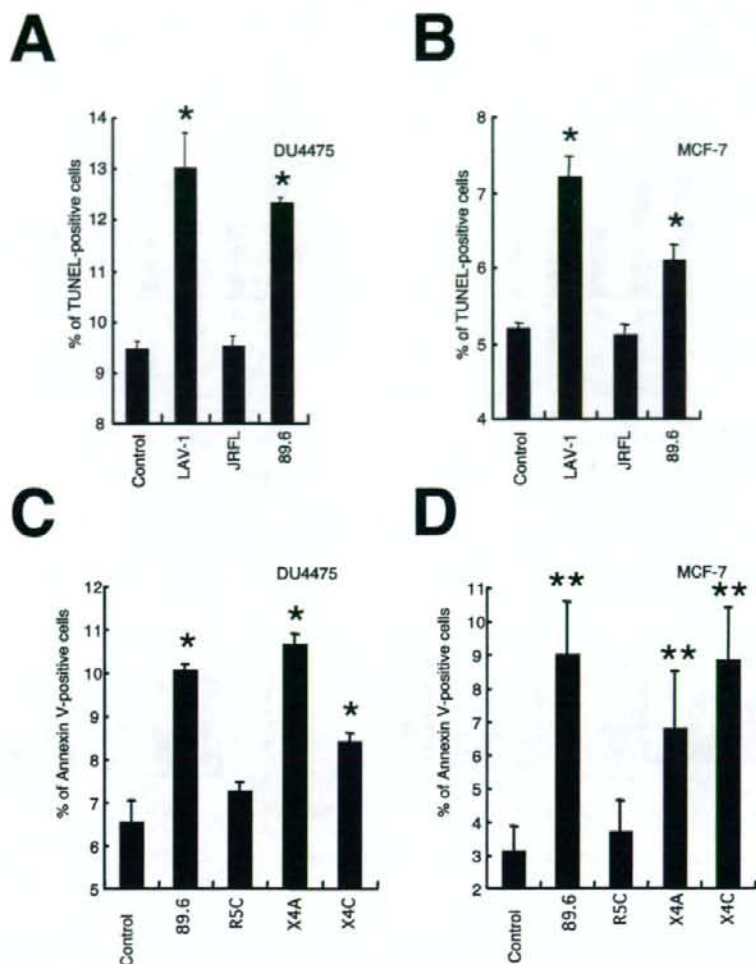


Fig. (3). Induction of apoptosis of breast cancer cells by HIV-1 is dependent on the HIV-1 phenotypic variants that are defined by their usage of CXCR4. DU4475 (A,C) and MCF-7 (B,D) cells were inoculated with the laboratory-adapted (X4 virus, HIV-1_{LAV-1}; R5 virus, HIV-1_{JRFL}; and R5X4 viruses, HIV-1_{89.6}) or primary HIV-1 isolates (R5 subtype C virus (R5C), HIV-1_{MU4}; X4 subtype A virus (X4A), HIV-1_{92UG029}; and X4 subtype C viruses (X4C), HIV-1_{98IND017}). For the control, the culture supernatant of uninfected cells was used. After a 36h incubation, the cells were subjected to TUNEL (A,B) or Annexin-V staining assay (C,D) to determine the percentage of apoptotic cells (* $p < 0.01$ compared with the control group, ** $p < 0.05$ compared with the control group (Dunnnett's test following ANOVA)).

CD4 antibody, an anti-CXCR4 antibody, or a CXCR4 antagonist, AMD3100, while HIV-1_{89.6} was also preincubated with a cross-reactive anti-gp120 antibody. The pretreatment of cells with 5 μ g of the anti-CXCR4 antibody 12G5 and 2 μ M AMD3100 significantly inhibited the apoptosis of DU4475 and MCF-7 cells (Fig. 4A,B). In contrast, the pretreatment with the isotype control or the anti-CD4 antibody had no effect on the apoptosis of breast cancer cells (Fig. 4A,B). Furthermore, the pretreatment of HIV-1_{89.6} with 5 μ g of the anti-gp120 antibody inhibited the apoptosis of breast cancer cells (Fig. 4A,B) and HIV-1_{89.6} gp120 induced the apoptosis of breast cancer cells (Fig. 4C). Taken together, these results demonstrated that the interaction of HIV-1

gp120 with CXCR4 is required for the induction of the apoptosis of breast cancer cells.

Next, we studied which intracellular signals were involved in HIV-1-associated breast cancer apoptosis. Vlahakis *et al.* demonstrated that HIV gp120/CXCR4-mediated CD4 T lymphocyte death occurs independent of $G_{i\alpha}$ protein action [34]. To determine whether CXCR4 signaling in breast cancer cells is similar to that in T-cell apoptosis, MCF-7 cells were preincubated with the $G_{i\alpha}$ protein inhibitor pertussis toxin before inoculation with HIV-1_{89.6}. Interestingly, breast cancer cell death was effectively blocked by pertussis toxin, suggesting that HIV-1 gp120/CXCR4-

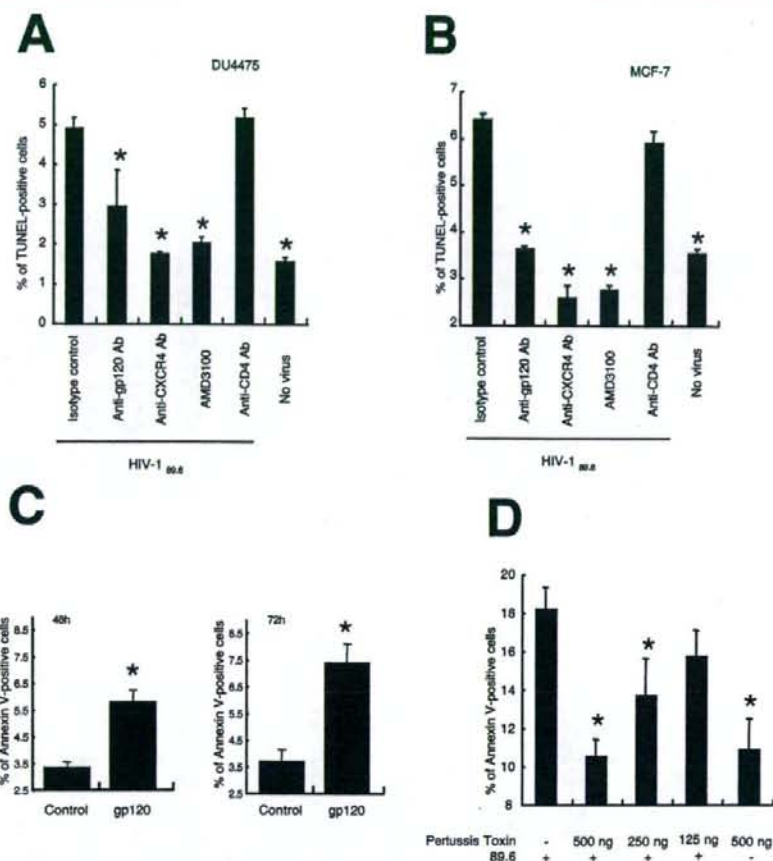


Fig. (4). HIV-1 induces breast cancer cell apoptosis through Env-CXCR4 interaction. DU4475 (A) and MCF-7 (B) cells were preincubated with 20 μ l of the anti-CD4 antibody (Leu-3a), 5 μ g of the anti-CXCR4 antibody (12G5), or 2 μ M CXCR4 antagonist (AMD3100) and then inoculated with HIV-1_{89.6} (100 ng of the HIV-1 p24 antigen). To prevent gp120-CXCR4 interaction, the virus that was preincubated with 5 μ g of the cross-reactive anti-gp120 antibody was also used. After a 36h incubation, the cells were subjected to TUNEL assay to determine the percentage of apoptotic cells (* p <0.01 compared with the isotype control group (Dunnett's test following ANOVA)). (C) Apoptosis of MCF-7 cells after 48h or 72h of coculture with HEK293 cells transfected with vector-derived mRNA (control) or mRNA encoding HIV-1_{89.6} gp120. MCF-7 cells were subjected to Annexin-V staining assay (* P <0.01 vs control, unpaired t test). (D) To investigate whether intracellular signaling is involved in HIV-1-associated breast cancer cell apoptosis, MCF-7 cells were preincubated with increasing concentrations of pertussis toxin, and inoculated with HIV-1_{89.6}. After a 36h incubation, the cells were subjected to Annexin-V staining assay (* p <0.01 compared with the control group without pertussis toxin (Dunnett's test following ANOVA)).

mediated apoptosis requires $G_{i\alpha}$ protein signaling in breast cancer cells (Fig. 4D).

Conformational Heterogeneity of CXCR4 on Cell Surface

To characterize CXCR4 on breast cancer and T cells, three conformation-specific anti-CXCR4 mAbs (12G5, 44717.111, and IA2-F9; [31, 35]) were used for flow cytometric analysis (Fig. 5). 12G5 recognizes a determinant in the first and second extracellular loops of CXCR4, and 44717.111 recognizes a determinant in the second extracellular loop (ECL-2) of CXCR4. Furthermore, IA2-F9 was previously generated in our laboratory by the immunization with a synthetic cyclic peptide that mimics the conformational specific domain of CXCR4 (UPA: Asn₁₇₆ to Ile₁₈₅). In breast cancer cells (DU4475 and MCF-7) and T cell

(Molt4#8), an anti-CXCR4 N-terminal rabbit polyclonal antibody (Fig. 1A) and IA2F9 (Fig. 5A,B) show almost equal reactivity. On the other hand, 12G5 and 44717.111 show high reactivity against CXCR4 on Molt4#8 cells but not on cells of breast cancer cell lines (Fig. 5A). Furthermore, other breast cancer cell lines (MDA-MB-231 and MDA-MB-453) were also analyzed for CXCR4 expression by flow cytometric analysis. As expected, 12G5 and 44717.111 hardly react with CXCR4 on cells of both cell lines (Fig. 5B). Taken together, these results suggest that both epitopes of 12G5 and 44717.111 are masked in breast cancer cells and that conformational differences in the microenvironment around ECL-2 plays an important role in the induction of HIV-1 gp120/CXCR4-mediated breast cancer apoptosis without CD4-induced conformational changes of gp120.

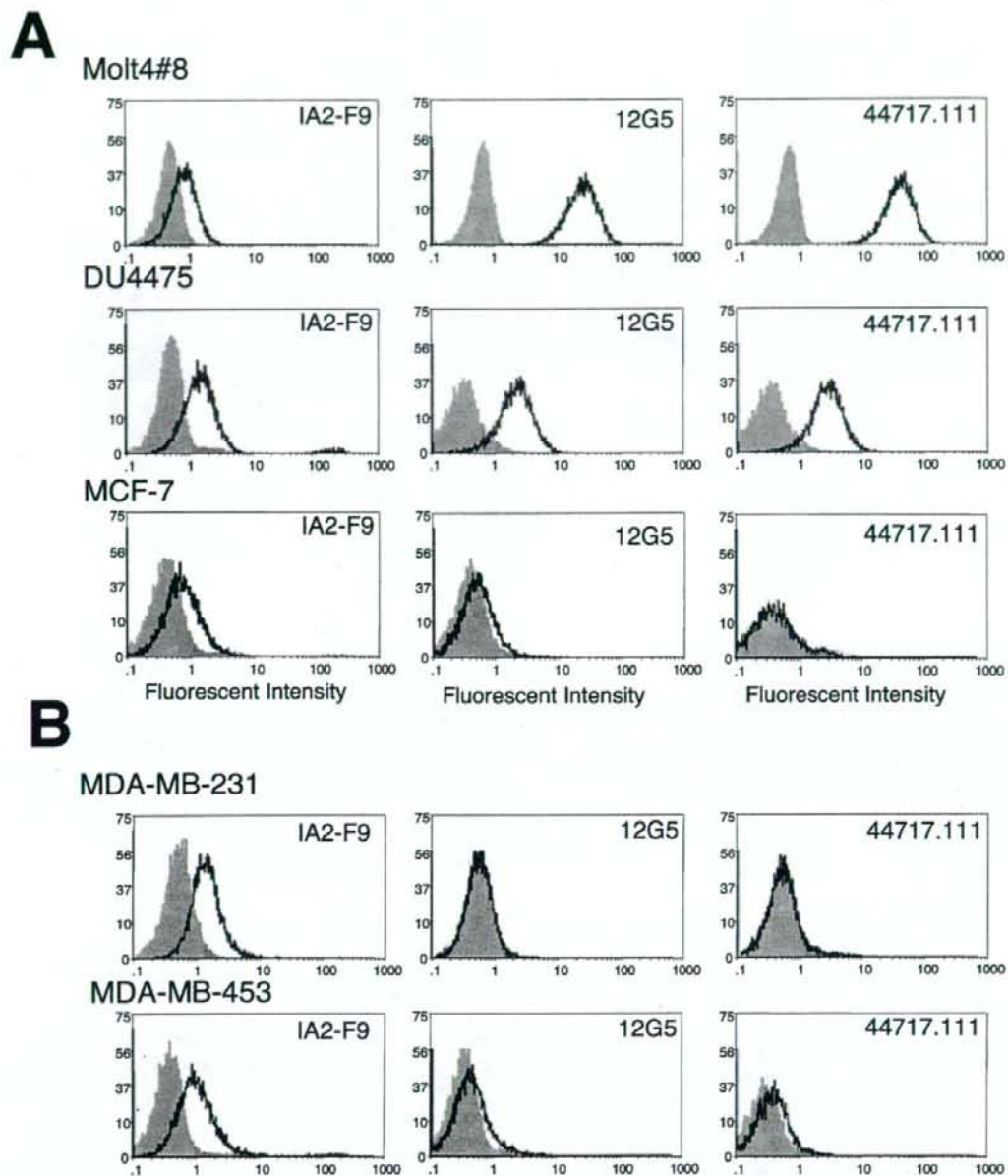


Fig. (5). Binding profile of conformation-specific anti-CXCR4 antibodies to T cell line and breast cancer cell lines. Human T-cell line (A, Molt4#8) and breast cancer cell lines (A, DU4475 and MCF-7; B, MDA-MB-231 and MDA-MB-453) were incubated with 10 μ g/ml conformation-specific anti-CXCR4 antibodies (12G5, 44717.111, and IA2F9; solid line), or isotype control (shadow). Subsequently, cells were incubated with suitable FITC-labeled secondary antibodies, and subjected to flow cytometry.

HIV-Induced Apoptosis of Breast Cancer Cells Via CXCR4 is Mediated by gp120 But Does Not Require CD4-Induced Conformational Change of gp120

Because DU4475 and MCF-7 cells do not express CD4 (Fig. 1B), we hypothesized that mutant gp120 (E370R) with a low CD4 binding ability [36] can specifically induce the

apoptosis of breast cancer cells. To test this hypothesis, gp120 (E370R)-expressing HEK293 cells were cocultured with MCF-7 or CEM cells. As expected, gp120 (E370R) can specifically induce the apoptosis of breast cancer cells (Fig. 6). This result indicates that the HIV-induced apoptosis of breast cancer cells *via* CXCR4 does not require a CD4-induced conformational change of gp120.

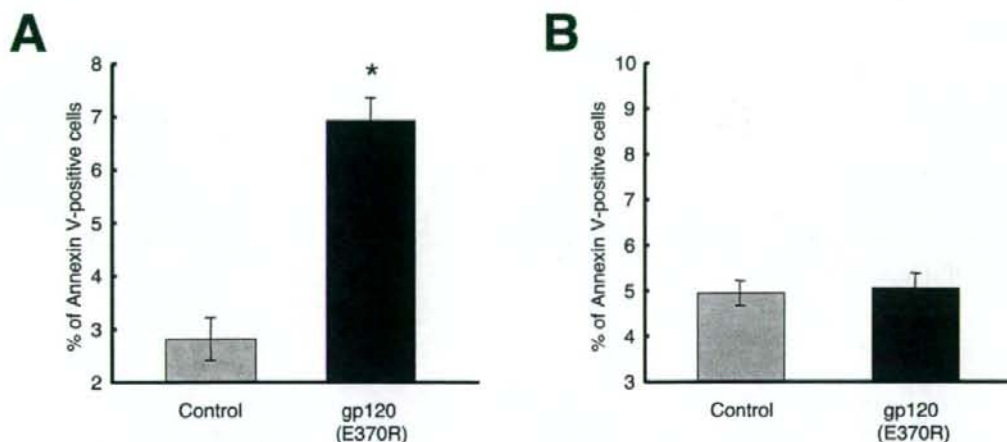


Fig. (6). CD4-induced conformational change in gp120 is not required to induce the apoptosis of breast cancer cells. Mutant gp120 (E370R, black) expressing and mock cells (gray) were seeded on polycarbonate Transwell filter inserts and cocultured with MCF-7 (A) or CEM (B) in the lower chamber. After 48h of coculture, MCF-7 cells or CEM cells were subjected to Annexin-V staining assay.

DISCUSSION

Because immunodeficiency fails to provide protection against viral infection or viral reactivation, the relative risks of HIV-1-associated cancers, particularly human-herpesvirus-8-associated Kaposi's sarcoma, and Epstein-Barr-virus-associated non-Hodgkin lymphoma, increase in HIV-1-infected patients [37-39]. On the other hand, the low incidence of breast cancer among HIV-1-infected patients has been reported by investigators from both African and Western countries [11, 41]. Several hypotheses explaining the low incidence of breast cancer among HIV-1-infected patients have been proposed (e.g., immunodeficiency, socioeconomic state, racial disparity, metabolic complications of antiretroviral therapy, and short life span of HIV-1-infected patients) [10-15]. On the basis of our data, we cannot exclude the possibility that HIV-1-induced breast cancer cell apoptosis is responsible for the reduced risk of breast cancer among HIV-1-infected patients, although further investigation is required.

In HIV-1-infected patients, soluble gp120 secreted by infected cells and gp120 expressed on virions or on the cell surface of infected cells can induce the apoptosis of uninfected T-cells [22]. The secreted and expressed gp120 can be considered as a ligand of CD4 and coreceptor molecules and may be involved in CD4- or CCR5-mediated Fas-dependent and CXCR4-mediated Fas-independent apoptosis [22]. As shown in Fig. (1), CXCR4 is expressed on human breast cancer cells; however, CD4 is hardly expressed. A recent study has shown that the degree of apoptosis of bystander T-cells induced by HIV-1 is associated with gp120-receptor affinity [25]. Therefore, we investigated whether HIV-1 can directly mediate the apoptosis of CD4-negative breast cancer cells. Our study showed that the induction of the apoptosis of breast cancer cells by HIV-1 is dependent on the viral strain. The laboratory-adapted and primary R5X4 and X4 viral isolates induced a high degree of apoptosis but not the R5 viral isolate.

We further demonstrated that the HIV-1-mediated apoptosis of breast cancer cells can be inhibited by using an anti-CXCR4 antibody and AMD3100. This indicates that CXCR4 is the major determinant of the HIV-1-induced apoptosis of breast cancer cells. Although Holm *et al.* proposed that the degree of apoptosis of bystander T-cells induced by HIV-1 is also associated with the coreceptor binding site exposure of gp120 induced by CD4 [25], breast cancer cell lines do not express CD4 molecules on the cell surface. However, as shown in Fig. 5, the conformational differences in the micro-environment around ECL-2 of CXCR4 on breast cancer cells may contribute to the direct gp120-CXCR4 interaction without the coreceptor binding site exposure of gp120.

As a type of effective oncolytic virotherapy for breast cancer, HIV-1 may be used to destroy breast cancer cells without harming healthy cells. To test this possibility, we prepared aldrithiol-2 (AT-2)-inactivated HIV-1 that has functional envelope glycoproteins but is not infectious. Interestingly, Annexin-V staining assay indicated that the percentage of apoptotic breast cancer cells significantly increased following the inoculation of AT-2-inactivated HIV-1_{89.6} (data not shown). However, it is difficult to use AT-2-inactivated HIV-1 for practical applications. Therefore, further structural optimization for mutant gp120 (E370R) that specifically induces the apoptosis of breast cancer cells may provide more efficient therapeutic information for developing a novel HIV-based breast cancer therapy.

At least 23 types of cancer cell express CXCR4 [41]. In addition, the relative risks of prostate, and bladder and breast cancer are significantly low in HIV-1-infected patients [36, 38]. Therefore, the low incidences of these cancers among HIV-1-infected patients may be involved in the emergence of R5X4 and X4 viruses *in vivo*. Further investigation of the effects of HIV-1 on these cancer cell types is necessary for elucidating the pathology of cancers and developing a novel HIV-based cancer therapy.

ACKNOWLEDGEMENTS

We thank the NIH AIDS Research and Reference Reagent Program for providing primary HIV-1 isolates (HIV-1_{MJ4}, HIV-1_{92UG029}, and HIV-1_{98IND17}), and AMD3100. We also thank the Cell Resource Center for Biomedical Research, Tohoku University for providing the breast cancer cell lines MCF-7, and SK-BR-3. This study was supported in part by a Grant-in-Aid for Scientific Research from the Ministry of Education, Culture, Sports, Science and Technology of Japan, and a Health Science Research Grant from the Ministry of Health, Labour, and Welfare of Japan.

REFERENCES

- [1] Fauci AS. The human immunodeficiency virus: infectivity and mechanisms of pathogenesis. *Science* 1988; 239: 617-622.
- [2] McCune JM. The dynamics of CD4+ T-cell depletion in HIV disease. *Nature* 2001; 410: 974-979.
- [3] Rabkin CS. AIDS and cancer in the era of highly active antiretroviral therapy (HAART). *Eur J Cancer* 2001; 37: 1316-1319.
- [4] Spano JP, Atlan D, Breau JI, *et al.* AIDS and non-AIDS-related malignancies: a new vexing challenge in HIV-positive patients. Part I: Kaposi's sarcoma, non-Hodgkin's lymphoma, and Hodgkin's lymphoma. *Eur J Intern Med* 2002; 13: 170-179.
- [5] Goedert JJ, Cote TR, Virgo P, *et al.* Spectrum of AIDS-associated malignant disorders. *Lancet* 1998; 351: 1833-1839.
- [6] Phelps RM, Smith DK, Heilig CM, *et al.* Cancer incidence in women with or at risk for HIV. *Int J Cancer* 2001; 94: 753-757.
- [7] Mbulaitye SM, Biggar RJ, Goedert JJ, *et al.* Immune deficiency and risk for malignancy among persons with AIDS. *J Acquir Immune Defic Syndr* 2003; 32: 527-533.
- [8] Remick SC. Non-AIDS-defining cancers. *Hematol Oncol Clin North Am* 1996; 10: 1203-1213.
- [9] Grulich AE, Li Y, McDonald A, *et al.* Rates of non-AIDS-defining cancers in people with HIV infection before and after AIDS diagnosis. *AIDS* 2002; 16: 1155-1161.
- [10] Herida M, Mary-Krause M, Kaphan R, *et al.* Incidence of non-AIDS-defining cancers before and during the highly active antiretroviral therapy era in a cohort of human immunodeficiency virus-infected patients. *J Clin Oncol* 2003; 21: 3447-3453.
- [11] Amir H, Kaaya EE, Kwasigabo G, *et al.* Breast cancer before and during the AIDS epidemic in women and men: a study of Tanzanian Cancer Registry Data 1968 to 1996. *J Natl Med Assoc* 2000; 92: 301-305.
- [12] Pantanowitz L, Dezube BJ. Reasons for a deficit of breast cancer among HIV-infected patients. *J Clin Oncol* 2004; 22: 1347-1348.
- [13] Dong KL, Bausserman LL, Flynn MM, *et al.* Changes in body habitus and serum lipid abnormalities in HIV-positive women on highly active antiretroviral therapy (HAART). *J Acquir Immune Defic Syndr* 1999; 21: 107-113.
- [14] Schreier LE, Berg GA, Basilio FM, *et al.* Lipoprotein alterations, abdominal fat distribution and breast cancer. *Biochem Mol Biol Int* 1999; 47: 681-690.
- [15] Krown SE. Breast cancer in the setting of HIV infection: cause for concern? *Cancer-Invest* 2002; 20(4): 590-592.
- [16] Moore JP, Trkola A, Dragic T. Co-receptors for HIV-1 entry. *Curr Opin Immunol* 1997; 9: 551-562.
- [17] Feng Y, Broder CC, Kennedy PE, *et al.* HIV-1 entry cofactor: functional cDNA cloning of a seven-transmembrane, G protein-coupled receptor. *Science* 1996; 272: 872-877.
- [18] Connor RI, Sheridan KE, Ceradini D, *et al.* Change in coreceptor use correlates with disease progression in HIV-1-infected individuals. *J Exp Med* 1997; 185: 621-628.
- [19] Scarlatti G, Tresoldi E, Bjornedal A, *et al.* *In vivo* evolution of HIV-1 co-receptor usage and sensitivity to chemokine-mediated suppression. *Nat Med* 1997; 3: 1259-1265.
- [20] Weissman D, Rabin RL, Arthos J, *et al.* Macrophage-tropic HIV and SIV envelope proteins induce a signal through the CCR5 chemokine receptor. *Nature* 1997; 389: 981-985.
- [21] Algeciras-Schimnich A, Vlahakis SR, Villasis-Keever A, *et al.* CCR5 mediates Fas- and caspase-8 dependent apoptosis of both uninfected and HIV infected primary human CD4 T cells. *AIDS* 2002; 16: 1467-1478.
- [22] Ahr B, Robert-Hebmann V, Devaux C, *et al.* Apoptosis of uninfected cells induced by HIV envelope glycoproteins. *Retrovirology* 2004; 1:12.
- [23] Berndt C, Mopps B, Angermuller S, *et al.* CXCR4 and CD4 mediate a rapid CD95-independent cell death in CD4(+) T cells. *Proc Natl Acad Sci USA* 1998; 95: 12556-12561.
- [24] Kreisberg JF, Kwa D, Schramm B, *et al.* Cytopathicity of human immunodeficiency virus type 1 primary isolates depends on coreceptor usage and not patient disease status. *J Virol* 2001; 75: 8842-8847.
- [25] Holm GH, Zhang C, Gorry PR, *et al.* Apoptosis of bystander T cells induced by human immunodeficiency virus type 1 with increased envelope/receptor affinity and coreceptor binding site exposure. *J Virol* 2004; 78: 4541-4551.
- [26] Herbein G, Mählkecht U, Batliwalla F, *et al.* Apoptosis of CD8+ T cells is mediated by macrophages through interaction of HIV gp120 with chemokine receptor CXCR4. *Nature* 1998; 395: 189-194.
- [27] Penn ML, Grivel JC, Schramm B, *et al.* CXCR4 utilization is sufficient to trigger CD4+ T cell depletion in HIV-1-infected human lymphoid tissue. *Proc Natl Acad Sci USA* 1999; 96: 663-668.
- [28] Jekle A, Schramm B, Jayakumar P, *et al.* Coreceptor phenotype of natural human immunodeficiency virus with nef deleted evolves *in vivo*, leading to increased virulence. *J Virol* 2002; 76: 6966-6973.
- [29] Muller A, Homey B, Soto H, *et al.* Involvement of chemokine receptors in breast cancer metastasis. *Nature* 2001; 410: 50-56.
- [30] Kato M, Kitayama J, Kazama S, *et al.* Expression pattern of CXCR4 chemokine receptor-4 is correlated with lymph node metastasis in human invasive ductal carcinoma. *Breast Cancer Res* 2003; 5: R144-150.
- [31] Misumi S, Endo M, Mukai R, *et al.* A novel cyclic peptide immunization strategy for preventing HIV-1/AIDS infection and progression. *J Biol Chem* 2003; 278: 32335-32343.
- [32] Remick SC, Harper GR, Abdullah MA, *et al.* Metastatic breast cancer in a young patient seropositive for human immunodeficiency virus. *J Natl Cancer Inst* 1991; 83: 447-448.
- [33] Samuelsson A, Brostrom C, van Dijk N, *et al.* Apoptosis of CD4+ and CD19+ cells during human immunodeficiency virus type 1 infection—correlation with clinical progression, viral load, and loss of humoral immunity. *Virology* 1997; 238: 180-188.
- [34] Vlahakis SR, Villasis-Keever A, Gomez TS, *et al.* Human immunodeficiency virus-induced apoptosis of human hepatocytes via CXCR4. *J Infect Dis* 2003; 188: 1455-1460.
- [35] Baribaud F, Edwards TG, Sharron M, *et al.* Antigenically distinct conformations of CXCR4. *J Virol* 2001; 75: 8957-8967.
- [36] Olshevsky U, Helseth E, Furman C, *et al.* Identification of individual human immunodeficiency virus type 1 gp120 amino acids important for CD4 receptor binding. *J Virol* 1990; 64: 5701-5707.
- [37] Gallagher B, Wang Z, Schymura MJ, *et al.* Cancer incidence in New York State acquired immunodeficiency syndrome patients. *Am J Epidemiol* 2001; 154: 544-556.
- [38] Biggar RJ, Kirby KA, Atkinson J, *et al.* Cancer risk in elderly persons with HIV/AIDS. *J Acquir Immune Defic Syndr* 2004; 36: 861-868.
- [39] Frisch M, Biggar RJ, Engels EA, *et al.* Association of cancer with AIDS-related immunosuppression in adults. *JAMA* 2001; 285: 1736-1745.
- [40] Pantanowitz L, Dezube BJ. Breast cancer in women with HIV/AIDS. *JAMA* 2001; 285: 3090-3091.
- [41] Balkwill F. The significance of cancer cell expression of the chemokine receptor CXCR4. *Semin Cancer Biol* 2004; 14: 171-179.

Modulation of Network-Driven, GABA-Mediated Giant Depolarizing Potentials by SDF-1 α in the Developing Hippocampus

Alexander Kasiyanov^{a-c} Nobutaka Fujii^d Hirokazu Tamamura^e
Huangui Xiong^{a-c}

^aNeurophysiology Laboratory, ^bCenter for Neurovirology and Neurodegenerative Disorders, and ^cDepartment of Pharmacology and Experimental Neuroscience, University of Nebraska Medical Center, Omaha, Nebr., USA; ^dGraduate School of Pharmaceutical Sciences, Kyoto University, Kyoto, and ^eDepartment of Molecular Recognition, Institute of Biomaterials and Bioengineering, Tokyo Medical and Dental University, Tokyo, Japan

Key Words

Chemokine · Chemokine CXC motif receptor 4 · Neurodevelopment · Hippocampal slices · Whole-cell recordings

Abstract

Chemokine stromal cell-derived factor-1 (SDF-1, or CXCL12) plays an important role in brain development and functioning. Whole-cell patch clamp recordings were conducted on CA3 neurons in hippocampal slices prepared from neonatal rats between postnatal days 2 and 6 to study the modulatory effects of SDF-1 α on network-driven, γ -aminobutyric acid-mediated giant depolarizing potentials (GDPs), a hallmark of the developing hippocampus. We found that SDF-1 α , the only natural ligand for chemokine CXC motif receptor 4 (CXCR4), decreased GDP firing without significant effects on neuronal passive membrane properties in neonatal hippocampal neurons. The SDF-1 α -mediated decrease in GDP firing was blocked by T140, a CXCR4 receptor antagonist, suggesting that SDF-1 α modulates GDP firing via CXCR4. We also showed that endogenous SDF-1 exerts a tonic inhibitory action on GDPs in the developing hippocampus. As SDF-1/CXCR4 are highly expressed in the developing brain

and GDPs are involved in activity-dependent synapse formation and functioning, the inhibitory action of SDF-1 α on GDPs may reflect a potential mechanism for chemokine regulation of neural development in early neonatal life.

Copyright © 2007 S. Karger AG, Basel

Introduction

An intriguing feature of neuronal activity in the developing nervous system is the presence of spontaneous rhythmic membrane oscillations termed giant depolarizing potentials (GDPs) [Ben-Ari et al., 1989]. GDPs are network-driven, and γ -aminobutyric acid (GABA)-mediated highly synchronized activity occurring at frequencies of 0.03–0.3 Hz. Characterized by recurrent membrane depolarization with superimposed fast action potentials [Ben-Ari et al., 1989; Bolea et al., 1999], GDPs can be detected in a wide range of brain structures including the hippocampus. They are believed to play an important role in activity-dependent synapse and network formation at early stages of brain development [Ben-Ari, 2001]. Like many other physiological activities, GDP is regulated by a number of neurotransmitters and mod-

KARGER

Fax +41 61 306 12 34
E-Mail karger@karger.ch
www.karger.com

© 2007 S. Karger AG, Basel

Accessible online at:
www.karger.com/dne

Huangui Xiong, MD, PhD
Department of Pharmacology and Experimental Neuroscience
Center for Neurovirology and Neurodegenerative Disorders
University of Nebraska Medical Center, Omaha, NE 68198-5880 (USA)
Tel. +1 402 559 5140, Fax +1 402 559 3744, E-Mail hxiong@unmc.edu

ulators. Recent studies have shown that chemokines (chemotactic cytokines) and their cognate receptors are highly expressed in a variety of brain regions during development and involved in regulating some of the developmental processes, such as neural cell migration, proliferation and survival in the developing brain [Banisadr et al., 2005; Tran et al., 2007]. Increasing evidence indicates that chemokines may modulate GDP activity in the developing brain.

Chemokines are a superfamily of small, secreted proteins (7–14 kDa) with diverse immune and neural functions [Mackay, 2001; Tran and Miller, 2003b]. They have been implicated in the development of the central and peripheral nervous systems [Tran and Miller, 2003b]. Four chemokine subfamilies, C, CC, CXC and CX3C, have so far been identified based on the relative position of conserved cysteine residues. Among chemokines and their cognate receptors with potential modulatory functions, stromal cell-derived factor-1 [SDF-1, also known as chemokine CXC motif ligand 12 (CXCL12)] and its cognate chemokine CXC motif receptor 4 (CXCR4) have attracted much attention.

SDF-1 belongs to the CXC subfamily and is the only known endogenous ligand for the receptor CXCR4, a G-protein-coupled receptor highly expressed in the immature brain. Studies have shown that SDF-1, by activating its cognate receptor CXCR4, regulates the migration of neural progenitor cells in the developing brain [Bagri et al., 2002; Schwarting et al., 2006; Tran et al., 2007] and modulates neural activities in diverse brain regions [Limatola et al., 2000; Liu et al., 2003; Callewaere et al., 2006; Guyon et al., 2006]. For example, SDF-1 modulates the firing pattern of vasopressin neurons in the hypothalamus [Callewaere et al., 2006] and the excitability of the substantia nigra dopaminergic neurons [Guyon et al., 2006]. SDF-1 can also modulate synaptic transmission in the hippocampus and cerebellum [Zheng et al., 1999; Guyon et al., 2006]. In addition, SDF-1 increases intracellular calcium in both human and rat neuronal cultures [Zheng et al., 1999; Limatola et al., 2000] and modulates synchronized Ca^{2+} spikes in hippocampal neurons [Liu et al., 2003]. These effects were mediated through the chemokine receptor CXCR4.

To understand the role that SDF-1/CXCR4 might play in neural plasticity and functioning, we studied the effects of SDF-1 α on GDPs recorded in the neonatal rat hippocampus. We found that SDF-1 α decreased the GDP firing via the receptor CXCR4 without changing basic synaptic activity. Application of the CXCR4 receptor antagonist T140 alone, on the other hand, increased the

GDP firing in a dose-dependent manner, suggesting that endogenous SDF-1 and the receptor CXCR4 are involved in modulating GDP firing in the immature rat hippocampus.

Materials and Methods

Chemicals

SDF-1 α was purchased from R & D Systems (Minneapolis, Minn., USA). Fura-2AM was obtained from Molecular Probes (Eugene, Oreg., USA). Neurobasal media were purchased from Invitrogen Corp. (Carlsbad, Calif., USA). 4F-benzoyl-TN14003 (T140) was obtained from Kyoto University (Sakyo-ku, Kyoto, Japan). All chemicals, unless otherwise specified, were from Sigma (St. Louis, Mo., USA).

Primary Hippocampal-Cortical Neuronal Cultures

Embryonic day 17–18 Sprague-Dawley rats were used for neuronal cultures. Hippocampal and cortical tissues were dissected out and were mechanically dissociated by trituration in a Ca^{2+}/Mg^{2+} -free Hank's balanced salt solution after 30 min of trypsin (0.1%) digestion at 37°C. Trypsin was neutralized with 10% fetal bovine serum (10%) and the cell suspension was washed three times in Hank's balanced salt solution and resuspended in neurobasal medium (Invitrogen Corp.) supplemented with 2 mM glutamine, 50 μ g/ml penicillin and streptomycin and B27. Cells were seeded on poly-D-lysine-coated cover slips at a concentration of 500,000 cells/ml. After 12–14 days in culture, the cells were used for Ca^{2+} imaging. The Institutional Animal Care and Use Committee (IACUC) of the University of Nebraska Medical Center strictly reviewed all animal use procedures (IACUC No. 00-062-07).

Ca^{2+} Imaging

Primary hippocampal-cortical neurons on cover slips were loaded with 5 μ M Fura-2AM at 27°C for 30 min. Cover slips were then transferred into a perfusion chamber (vol. = 1 ml) mounted on the stage of an inverted Nikon TMD Diaphot epifluorescent microscope ($\times 40$ water immersion lens). The cells were perfused (1 ml/min) with artificial cerebrospinal fluid (ACSF) containing (in mM): NaCl 130.0, KCl 3.5, $CaCl_2$ 2.0, $MgCl_2$ 1.3, NaH_2PO_4 1.2, $NaHCO_3$ 26.0, and glucose 10.0, pH 7.4, after saturation with 95% $O_2/5\%$ CO_2 . Intracellular Ca^{2+} imaging was made at room temperature. The Fura-2 fluorescence of individual neuronal cells was captured using a digital camera (Photometrics, Huntington Beach). Axon Imaging Workbench-2 (Axon Instrument) was employed for excitation control, image acquisition and off-line analysis. Neuronal cells were selected based on their morphology and analyzed independently for each time point in the captured sequence. Excitation and emission wavelengths were 340/380 nm and 500 nm, respectively.

Hippocampal Slice Preparation

Hippocampal brain slices were prepared from Sprague-Dawley rats of either sex between postnatal day (P) 2 and P6 as described previously [Kasyanov et al., 2004]. Briefly, animals were anesthetized with isoflurane and surgically decapitated. The brain was quickly removed from the skull and submerged in

ACSF containing (in mM): NaCl 126.0, KCl 3.5, CaCl₂ 2.0, MgCl₂ 1.3, NaH₂PO₄ 1.2, NaHCO₃ 25.0, glucose 11, and saturated with 95% O₂ and 5% CO₂ (pH 7.4). Coronal hippocampal slices (500 μm in thickness) were cut with a motorized vibroslicer (WPI, Sarasota, Fla., USA) and incubated at room temperature in oxygenated ACSF for at least 1 h before use.

Electrophysiology

For whole-cell patch recordings, individual slices were transferred to the recording chamber and superfused with ACSF at 2.5–3.0 ml min⁻¹ at 34°C. Whole-cell recordings were performed on CA3 pyramidal cells in hippocampal slices using a 'blind' method. Spontaneous GDPs and excitatory postsynaptic potentials were recorded and amplified using an Axopatch-1D amplifier (Axon Instruments, Union City, Calif., USA), filtered at 1 kHz, and digitized at 5 kHz through a Digidata 1322A digitizer (Axon Instruments). To minimize potential 'contamination' of the excitatory postsynaptic potentials by spontaneous action potentials, the cells were hyperpolarized to -80 mV. pCLAMP 8 software was used for data acquisition (gap-free configuration). Patch electrodes were made from borosilicate glass capillaries (WPI) and had a resistance of 5–7 MΩ when filled with intracellular solution containing (in mM): KCl 140, HEPES 10, EGTA 1, MgCl₂ 1, MgATP 2 (pH 7.3 after adjustment with KOH, osmolarity 280–290 mosm). The whole-cell capacitance was fully compensated and the series resistance (10–20 MΩ) was compensated at 75–80%. Membrane input resistance was calculated by measuring membrane voltage change in response to a small hyperpolarizing current pulse (300 ms in duration) across the cell membrane. Series resistance was monitored throughout the recordings. A cell was discarded if it changed significantly (>20% of the control). Both pCLAMP 8 and Mini Analysis Program (Synaptosoft Inc., Decatur, Ga., USA) were employed for data analysis. For each cell, the mean GDP frequency was calculated in control conditions and during drug application (starting 1 min after the onset of drug perfusion). Statistical comparisons were made between mean values (control vs. drug treatment). The numerical data are given as mean ± SEM and compared using Student's *t* test. The differences were considered significant when *p* < 0.05.

Results

Under whole-cell patch recording the neonatal hippocampal CA3 neurons fired spontaneous GDPs which occurred randomly at a frequency of 0.102 ± 0.003 Hz (*n* = 22). The spontaneous GDPs were blocked either by the GABA_A receptor antagonist picrotoxin (100 μM, *n* = 5) or by the Na⁺ channel blocker tetrodotoxin (0.1 μM, *n* = 5), but not by the NMDA receptor antagonist 2-amino-5-phosphovalerate (50 μM, *n* = 5, data not shown). These results suggest that GDPs were GABA-mediated, network-driven events. Blended with GDPs were spontaneous mini-synaptic potentials (SMSPs). To determine whether chemokine SDF-1 influences GDPs, we studied the effects of SDF-1α on GDP firing in neonatal rat hip-

pocampal CA3 pyramidal cells. Bath application of SDF-1α produced a decrease in GDP firing (fig. 1a, b) in a concentration-dependent manner (fig. 1c). At a concentration of 5 nM, SDF-1α induced a slight reduction of GDP frequency (fig. 1c; *n* = 5). However, it produced a remarkable (*p* < 0.05) decrease in GDP frequency at a concentration of 50 nM, from 0.112 ± 0.005 Hz to 0.061 ± 0.010 Hz (*n* = 7), followed by a slight increase during the washout period with a firing frequency of 0.133 ± 0.007 Hz (*n* = 7) (fig. 1a, b). The SDF-1α-induced decrease in GDP firing was rapid in onset and reached the maximum in 2–3 min, it usually recovered in 5–10 min. The SDF-1α-associated reduction of GDP frequency was not accompanied by changes of either the membrane potential or membrane input resistance. The average membrane potentials before and after application of SDF-1α were -79.7 ± 5.1 mV and -81.4 ± 8.2 mV (*n* = 5), respectively, and the membrane input resistance was 99.1 ± 7.2% of basal level before application of SDF-1α and 107 ± 18.7% of basal level (*n* = 5) during the washout period. The differences were not statistically significant (*p* > 0.05). While decreasing GDP firing frequency, the SDF-1α had no significant effects on SMSPs as assayed by analyzing the frequency and amplitude of the SMSPs. The amplitudes and frequencies of SMSPs before and after application of SDF-1α were 8.8 ± 2.2 mV and 9.3 ± 1.9 mV, respectively, and 2.70 ± 1.27 Hz and 3.26 ± 1.66 Hz, respectively. Statistical analyses showed no significant differences on either amplitude or frequency (*p* > 0.05, *n* = 5), indicating that SDF-1α had no significant effects on basal synaptic transmission.

As CXCR4 receptors are expressed in the hippocampus and the SDF-1 is the only ligand for CXCR4, we examined whether SDF-1α-induced reduction of GDPs was mediated via CXCR4 by using T140, an antagonist for CXCR4. The GDP frequency recorded in CA3 neurons was 0.061 ± 0.010 Hz (*n* = 7) when hippocampal slices were superfused with SDF-1α (50 nM). In contrast, the GDP frequency was 0.080 ± 0.004 Hz when slices were superfused with both T140 and SDF-1α (fig. 2; *n* = 5). The difference was statistically significant, suggesting a blockade of the SDF-1α-associated reduction of GDP frequency by T140. These results also suggest that CXCR4 receptors are present and functional at an early stage of development.

It has been shown that SDF-1α/CXCR4 play a role in the development of the hippocampus [Lu et al., 2002; Lazarini et al., 2003]. We hypothesize that endogenous SDF-1α released from neuroglial cells might modulate CA3 neuronal activity in the developing hippocampus. To test

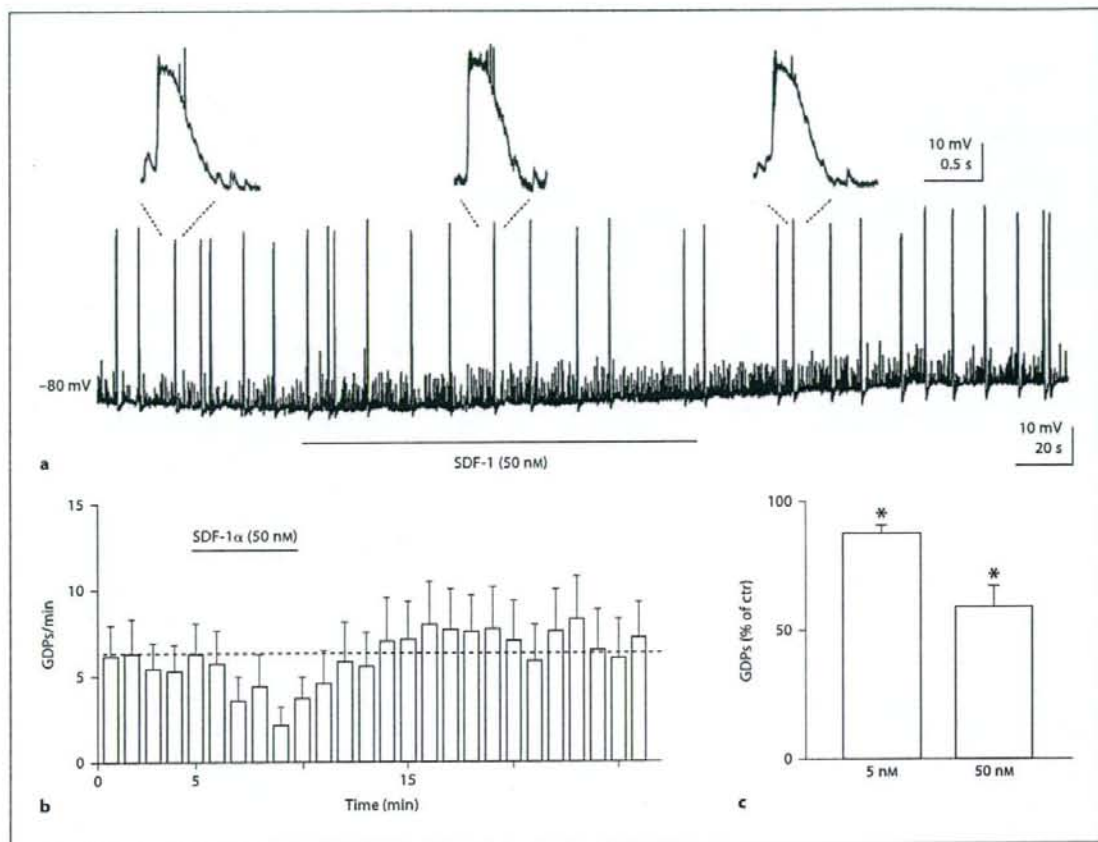


Fig. 1. SDF-1 α decreases GDP firing in rat hippocampal slices. **a** A representative trace recorded from a CA3 pyramidal neuron in a hippocampal slice prepared from a neonatal rat at P4. The horizontal bar below the trace indicates bath application of SDF-1 α (50 nM). Three individual GDPs, taken before, during and after bath application of SDF-1 α , are shown above the trace at an expanded time scale. **b** The time course illustrating the average GDP frequency before, during, and after application of SDF-1 α (horizontal bar) as a function of time for 7 cells. Each column repre-

sents the number of GDPs recorded in 1 min. The broken line represents the mean GDP frequency under control conditions. **c** A summarized bar graph showing concentration-dependent reduction of the GDP frequency caused by SDF-1 α . Each bar represents the percentage of the GDP frequency recorded during bath application of SDF-1 α at 5 nM ($n = 5$) and 50 nM ($n = 7$), respectively. The percentage was calculated in comparison with the GDP frequency recorded during the control (ctr) period, which was treated as 100%. * $p < 0.05$.

our hypothesis, we investigated the effects of the CXCR4 receptor antagonist T140 on GDPs in CA3 neuronal cells in rat hippocampal slices. Bath application of T140 revealed a concentration-dependent increase in GDP frequency. At 50 nM, T140 had no significant effect on GDPs. However, at a concentration of 500 nM, T140 significantly enhanced the frequency of GDPs from 0.09 ± 0.02 Hz to 0.15 ± 0.04 Hz (fig. 3; $n = 7$, $p < 0.05$), indicating that

endogenous SDF-1 exerts an inhibitory action on GDPs. Further analysis revealed that T140 had no significant effects on either the shape of GDPs or the amplitude of SMSPs (data not shown).

GDPs induce intracellular Ca^{2+} oscillation [Leinekugel et al., 1995], a cellular event which may be associated with synaptic formation and development. To find out whether the modulatory action of SDF-1 α on GDPs is ac-

Fig. 2. Blockade of SDF-1 α -mediated reduction of GDP firing by T140, a CXCR4 receptor antagonist. Each column represents the number of GDPs recorded in 1 min. The dashed line represents the mean GDP frequency under control conditions. Bath application of T140 (500 nM) is indicated by a long horizontal bar and bath application of SDF-1 α (50 nM) is represented by a short horizontal bar. Note that T140 abolished SDF-1 α -associated reduction of GDP firing frequency.

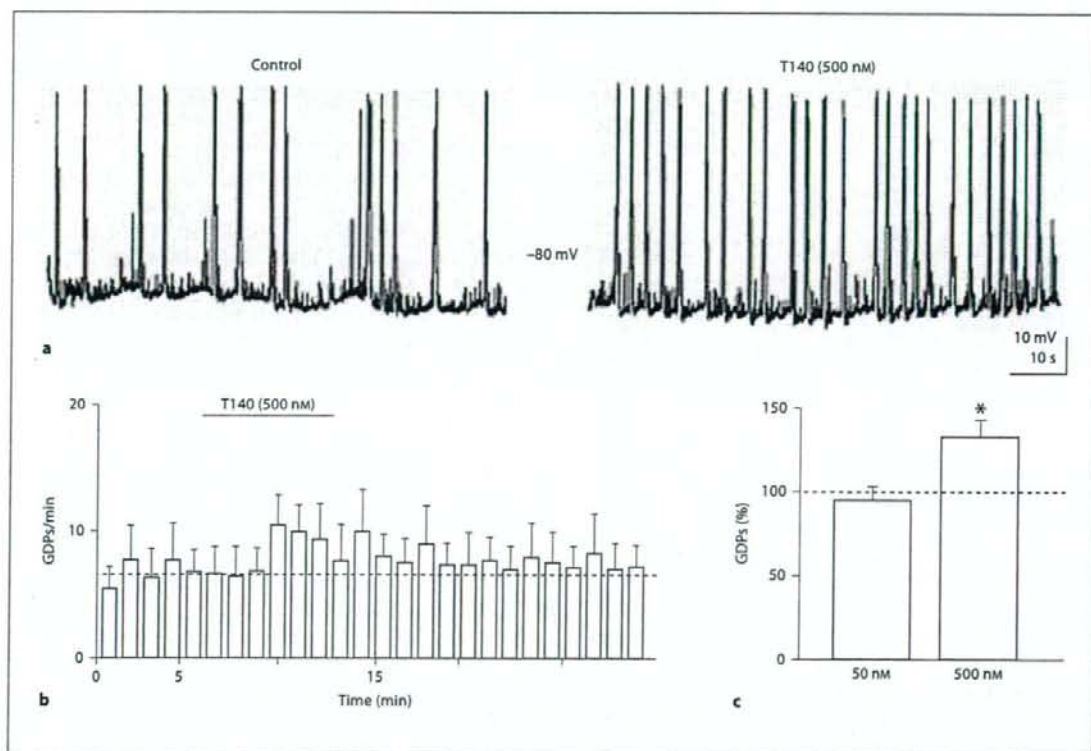
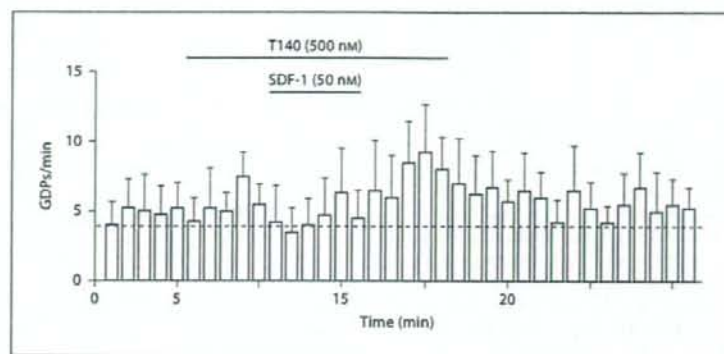
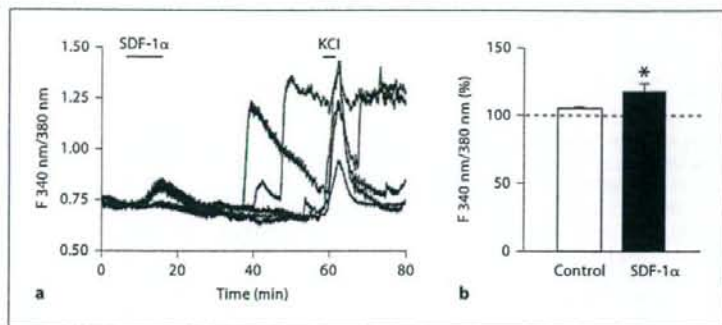


Fig. 3. Application of the CXCR4 receptor antagonist alone enhanced GDP firing. **a** Representative traces recorded from a CA3 neuron before (left) and during (right) bath application of T140. Note that T140 enhanced GDP firing. **b** The plot of an average GDP frequency as a function of time for 7 cells. Each column represents the number of GDPs recorded in 1 min. The dashed line

represents the mean GDP frequency under control conditions. The horizontal bar indicates the time of bath application of T140 (500 nM). **c** A summarized bar graph illustrating the relationship of average GDP frequency as a function of T140 concentrations. Each bar represents the percentage of changing of the GDP frequency induced by T140 at different concentrations.

Fig. 4. SDF-1 α produced a delayed elevation of intracellular Ca²⁺ levels in primary hippocampal-cortical neuronal cultures. **a** Representative traces (n = 5) of calcium imaging after application and washout of SDF-1 α . KCl (1 M) was applied for verification of neuronal cells. **b** The average of the fluorescence ratio measured during application of SDF-1 α and 30–50 min after washout of SDF-1 α (n = 16). * p < 0.05.



accompanied by intracellular Ca²⁺ oscillation, we monitored the dynamic changes of [Ca²⁺]_i in primary hippocampal-cortical neuronal cultures. We found that SDF-1 α induced a delayed increase in [Ca²⁺]_i, with an average fluorescence ratio of 121.5 ± 7.5%. In comparison with the fluorescence ratio in untreated controls, the difference was statistically significant (fig. 4; p < 0.05, n = 16).

Discussion

In this study, we have demonstrated that chemokine SDF-1 α dose-dependently inhibited GDP firing of CA3 pyramidal cells in hippocampal slices prepared from neonatal rats. The SDF-1 α -mediated inhibition on GDPs was blocked by the CXCR4 receptor antagonist, indicating that SDF-1 α inhibits GDPs via the chemokine receptor CXCR4. Further investigation revealed that endogenous SDF-1 exerts a tonic inhibition on GDPs as evidenced by the experimental results that bath application of the CXCR4 receptor antagonist alone led to an enhancement of GDP activity. These data suggest that SDF-1 α /CXCR4 may function as a neuromodulator early in postnatal life.

Unlike many other chemokines and their receptors, SDF-1 and its receptor CXCR4 are expressed not only in the peripheral blood and organs [Bleul et al., 1997] but also in the brain on a variety of cell types, including microglia, astrocytes, and neurons [Lavi et al., 1998; Albright et al., 1999; Stumm et al., 2003], as well as embryonic and adult neural progenitor cells [Tran et al., 2004]. The expression of SDF-1 α /CXCR4 in both hematopoietic organs and proliferative areas of the brain [Jazin et al., 1997] suggests an important role for SDF-1/CXCR4 in diverse cellular aspects during development. Accumulating

evidence indicates that CXCR4 and its unique ligand SDF-1 play a central role not only in the immune system but also in the developing and mature nervous system where they modulate cell migration, growth and neural development [Bagri et al., 2002; Belmadani et al., 2005]. Indeed, it has been shown that modulation of neural development by SDF-1 α /CXCR4 takes place in the cerebellum and hippocampus. In vivo studies indicate that SDF-1 α /CXCR4 influence cerebellar development by modulating both the migration and proliferation of cerebellar granule cells [Zou et al., 1998]. The involvement of SDF-1 α /CXCR4 in hippocampal development is revealed by experiments demonstrating that mice lacking CXCR4 receptors have abnormal development of the hippocampal dentate gyrus [Bagri et al., 2002; Lu et al., 2002]. In addition, SDF-1 α has been shown to modulate neuronal excitability, synaptic transmission and neuroendocrine activity [Limatola et al., 2000; Callewaere et al., 2006; Guyon et al., 2006]. In the present study, we showed that SDF-1 α modulates network-driven, GABA-mediated GDPs via the receptor CXCR4 in the CA3 pyramidal cells in neonatal rat hippocampal slices. These results collectively demonstrate a neuromodulatory role for SDF-1/CXCR4 in the central nervous system.

A striking feature in the developing hippocampus is the presence of spontaneous rhythmic-like neuronal oscillations, the GDPs. These neuronal oscillations are recurrent network-driven synaptic events generated by GABA, which in neonatal life is depolarizing and excitatory [Ben-Ari et al., 1989]. The GDPs we recorded in the CA3 area were blocked either by tetrodotoxin or by the GABA_A receptor antagonist picrotoxin, but not by the NMDA receptor antagonist 2-amino-5-phosphovalerate, suggesting that the GDPs we recorded are network-driven, GABA-mediated events as reported by others [Ben-

Ari et al., 1989). GDPs enable a high degree of synchrony in immature neurons in spite of the small number of functional synapses and participate in activity-dependent growth and synapse formation [Ben-Ari, 2001]. They are subject to modulation by endogenous and/or exogenous substances such as neurotransmitters and/or chemokines. One of the most likely modulators is SDF-1, as SDF-1 and its receptor CXCR4 are highly expressed in the central nervous system cells during development [Tham et al., 2001; Tran and Miller, 2003a]. Our results showed that bath application of SDF-1 α decreased GDP firing and this decrease was blocked by T140, a CXCR4 receptor antagonist. Moreover, application of T140 alone led to an increase in spontaneous GDPs, indicating that endogenous SDF-1 exerts a tonic inhibitory action on GDP firing. These results support a role for SDF-1 α /CXCR4 in modulating GDPs in the developing hippocampus.

As CXCR4 is expressed in both glial and neuronal cells [Albright et al., 1999; Stumm et al., 2003], bath-applied SDF-1 α may interact with the CXCR4 receptors expressed on all types of neural cells. Our results showed that SDF-1 α decreases GDPs without a significant alteration of the membrane potential and membrane input resistance. This suggests that the site of action for SDF-1 α may be on neuronal network and/or other neural cells other than the soma of recorded CA3 pyramidal cells. It is possible that SDF-1 α acts on GABAergic interneurons and decreases GABAergic interneuron release of GABA, resulting in a reduction of GDPs. It may also be that SDF-1 α acts on neural network, leading to a suppression of GDP firing in CA3 neurons in the developing hippocampus.

There are at least two distinct mechanisms of GDP generation in the hippocampus. One of them is that excitatory GABAergic interneurons release GABA onto pyramidal cells and participate in a positive feedback loop on the synchronous discharge of a population of pyramidal cells [Ben-Ari et al., 1989]. Thus, increase in GABA release from interneurons is sufficient to synchronize the entire network and to induce GDPs. The other mechanism emphasizes that the source of the generation of GDPs in the developing hippocampus is the spontaneous oscillation of intracellular Ca²⁺ concentration in pacemaker cells [Strata et al., 1997; Liu et al., 2003]. Such oscillations are found in many types of neural tissues in vivo and in vitro, ranging from the hippocampus to the visual system [Gu et al., 1994; Spitzer, 1994; Leinekugel et al., 1999]. It is possible that SDF-1 α has the potential to modulate GDP firing through either of these mechanisms. However, our Ca²⁺ imaging results showed that

the time course for the SDF-1 α -induced increase in [Ca²⁺]_i did not match the time course of the SDF-1 α -mediated decrease in GDP firing, suggesting that SDF-1 α modulation of GDPs via influence of [Ca²⁺]_i was less likely. Thus, we propose that the SDF-1 α -mediated decrease in GDPs is most likely the consequence of SDF-1 α inhibition of GABA release from GABAergic neurons.

The expression of SDF-1 α /CXCR4 in nonhematopoietic cells, such as neurons and astrocytes, suggests that this chemokine and its receptor have other roles in addition to leukocyte chemotaxis [Bacon and Harrison, 2000]. Studies have shown that CXCR4 signaling causes a wide range of biological effects in the central nervous system. Animals lacking CXCR4, for example, were found to exhibit abnormal development of the hippocampal dentate gyrus [Lu et al., 2002]. Our experiments with T140 clearly demonstrate that endogenous SDF-1 α is involved in the modulation of GDP firing. As GDPs are innate, network-driven rhythmic activities in the developing hippocampus, the inhibitory effects of SDF-1 α on GDPs may represent an important role that SDF-1 α /CXCR4 might play in regulating neuronal and synaptic development in the developing nervous system. It may also be that SDF-1 α stimulates glial cells to release other cytokines/chemokines, which in turn influence GABA-mediated synaptic events or change the feature of 'pacemaker' cells in the immature hippocampus, or both.

Acknowledgements

This study was supported by NIH grant R01 NS041862 to H.X. We thank Dr. Mark Thomas, Ms. Robin Taylor and Mr. James Keblesh for reading the manuscript.

References

- Albright AV, Shieh JT, Itoh T, Lee B, Pleasure D, O'Connor MJ, Doms RW, Gonzalez-Scarano F (1999): Microglia express CCR5, CXCR4, and CCR3, but of these, CCR5 is the principal coreceptor for human immunodeficiency virus type 1 dementia isolates. *J Virol* 73: 205-213.
- Bacon KB, Harrison JK (2000): Chemokines and their receptors in neurobiology: perspectives in physiology and homeostasis. *J Neuroimmunol* 104:92-97.
- Bagri A, Gurney T, He X, Zou YR, Littman DR, Tessier-Lavigne M, Pleasure SJ (2002): The chemokine SDF1 regulates migration of dentate granule cells. *Development* 129:4249-4260.

- Banisadr G, Rostene W, Kitabgi P, Parsadaniantz SM (2005): Chemokines and brain functions. *Curr Drug Targets Inflamm Allergy* 4: 387-399.
- Belmadani A, Tran PB, Ren D, Assimakopoulos S, Grove EA, Miller RJ (2005): The chemokine stromal cell-derived factor-1 regulates the migration of sensory neuron progenitors. *J Neurosci* 25:3995-4003.
- Ben-Ari Y (2001): Developing networks play a similar melody. *Trends Neurosci* 24:353-360.
- Ben-Ari Y, Cherubini E, Corradetti R, Gaiarsa JL (1989): Giant synaptic potentials in immature rat CA3 hippocampal neurons. *J Physiol* 416:303-325.
- Bleul CC, Wu L, Hoxie JA, Springer TA, Mackay CR (1997): The HIV coreceptors CXCR4 and CCR5 are differentially expressed and regulated on human T lymphocytes. *Proc Natl Acad Sci USA* 94:1925-1930.
- Bolea S, Avignone E, Berretta N, Sanchez-Andres JV, Cherubini E (1999): Glutamate controls the induction of GABA-mediated giant depolarizing potentials through AMPA receptors in neonatal rat hippocampal slices. *J Neurophysiol* 81:2095-2102.
- Callewaere C, Banisadr G, Desarmenien MG, Mechighel P, Kitabgi P, Rostene WH, Melik Parsadaniantz S (2006): The chemokine SDF-1/CXCL12 modulates the firing pattern of vasopressin neurons and counteracts induced vasopressin release through CXCR4. *Proc Natl Acad Sci USA* 103:8221-8226.
- Gu X, Olson EC, Spitzer NC (1994): Spontaneous neuronal calcium spikes and waves during early differentiation. *J Neurosci* 14:6325-6335.
- Guyon A, Skrzydelski D, Rovere C, Rostene W, Parsadaniantz SM, Nahon JL (2006): Stromal cell-derived factor-1alpha modulation of the excitability of rat substantia nigra dopaminergic neurons: presynaptic mechanisms. *J Neurochem* 96:1540-1550.
- Jazin EE, Soderstrom S, Ebendal T, Larhammar D (1997): Embryonic expression of the mRNA for the rat homologue of the fusin/CXCR-4 HIV-1 co-receptor. *J Neuroimmunol* 79:148-154.
- Kasyanov AM, Safulina VF, Voronin LL, Cherubini E (2004): GABA-mediated giant depolarizing potentials as coincidence detectors for enhancing synaptic efficacy in the developing hippocampus. *Proc Natl Acad Sci USA* 101:3967-3972.
- Lavi E, Kolson DL, Ulrich AM, Fu L, Gonzalez-Scarano F (1998): Chemokine receptors in the human brain and their relationship to HIV infection. *J Neurovirol* 4:301-311.
- Lazarini F, Tham TN, Casanova P, Arenzana-Seisdedos F, Dubois-Dalcq M (2003): Role of the alpha-chemokine stromal cell-derived factor (SDF-1) in the developing and mature central nervous system. *Glia* 42:139-148.
- Leinekugel X, Khalilov I, McLean H, Caillard O, Gaiarsa JL, Ben-Ari Y, Khazipov R (1999): GABA is the principal fast-acting excitatory transmitter in the neonatal brain. *Adv Neurol* 79:189-201.
- Leinekugel X, Tseeb V, Ben-Ari Y, Bregestovski P (1995): Synaptic GABA_A activation induces Ca²⁺ rise in pyramidal cells and interneurons from rat neonatal hippocampal slices. *J Physiol* 487:319-329.
- Limatola C, Giovannelli A, Maggi L, Ragozzino D, Castellani L, Ciotti MT, Vacca F, Mercanti D, Santoni A, Eusebi F (2000): SDF-1alpha-mediated modulation of synaptic transmission in rat cerebellum. *Eur J Neurosci* 12: 2497-2504.
- Liu Z, Geng L, Li R, He X, Zheng JQ, Xie Z (2003): Frequency modulation of synchronized Ca²⁺ spikes in cultured hippocampal networks through G-protein-coupled receptors. *J Neurosci* 23:4156-4163.
- Lu M, Grove EA, Miller RJ (2002): Abnormal development of the hippocampal dentate gyrus in mice lacking the CXCR4 chemokine receptor. *Proc Natl Acad Sci USA* 99:7090-7095.
- Mackay CR (2001): Chemokines: immunology's high impact factors. *Nat Immunol* 2:95-101.
- Schwartz GA, Henion TR, Nugent JD, Caplan B, Tobet S (2006): Stromal cell-derived factor-1 (chemokine C-X-C motif ligand 12) and chemokine C-X-C motif receptor 4 are required for migration of gonadotropin-releasing hormone neurons to the forebrain. *J Neurosci* 26:6834-6840.
- Spitzer NC (1994): Spontaneous Ca²⁺ spikes and waves in embryonic neurons: signaling systems for differentiation. *Trends Neurosci* 17: 115-118.
- Strata F, Atzori M, Molnar M, Ugolini G, Tempia F, Cherubini E (1997): A pacemaker current in dye-coupled hilar interneurons contributes to the generation of giant GABAergic potentials in developing hippocampus. *J Neurosci* 17:1435-1446.
- Stumm RK, Zhou C, Ara T, Lazarini F, Dubois-Dalcq M, Nagasawa T, Holt V, Schulz S (2003): CXCR4 regulates interneuron migration in the developing neocortex. *J Neurosci* 23:5123-5130.
- Tham TN, Lazarini F, Franceschini IA, Lachapelle F, Amara A, Dubois-Dalcq M (2001): Developmental pattern of expression of the alpha chemokine stromal cell-derived factor 1 in the rat central nervous system. *Eur J Neurosci* 13:845-856.
- Tran PB, Banisadr G, Ren D, Chenn A, Miller RJ (2007): Chemokine receptor expression by neural progenitor cells in neurogenic regions of mouse brain. *J Comp Neurol* 500:1007-1033.
- Tran PB, Miller RJ (2003a): Chemokine receptors in the brain: a developing story. *J Comp Neurol* 457:1-6.
- Tran PB, Miller RJ (2003b): Chemokine receptors: signposts to brain development and disease. *Nat Rev Neurosci* 4:444-455.
- Tran PB, Ren D, Veldhouse TJ, Miller RJ (2004): Chemokine receptors are expressed widely by embryonic and adult neural progenitor cells. *J Neurosci Res* 76:20-34.
- Zheng J, Thylin MR, Ghorpade A, Xiong H, Persidsky Y, Cotter R, Niemann D, Che M, Zeng YC, Gelbard HA, Shepard RB, Swartz JM, Gendelman HE (1999): Intracellular CXCR4 signaling, neuronal apoptosis and neuro-pathogenic mechanisms of HIV-1-associated dementia. *J Neuroimmunol* 98:185-200.
- Zou YR, Kottmann AH, Kuroda M, Taniuchi I, Littman DR (1998): Function of the chemokine receptor CXCR4 in haematopoiesis and in cerebellar development. *Nature* 393:595-599.

Development of Peptide-targeted Lipoplexes to CXCR4-expressing Rat Glioma Cells and Rat Proliferating Endothelial Cells

Wouter HP Driessen¹, Nobutaka Fujii², Hirokazu Tamamura³ and Sean M Sullivan^{1*}

¹Department of Pharmaceutical Sciences, College of Pharmacy, University of Florida, Gainesville, Florida, USA; ²Department of Biorganic Medicinal Chemistry Graduate School of Pharmaceutical Sciences, Kyoto University, Yoshida Shimoadachi-cho, Kyoto, Japan; ³Institute of Biomaterials and Bioengineering, Tokyo Medical and Dental University, Tokyo, Japan

A peptide analog, 4-fluorobenzoyl-RR-(L-3-(2-naphthyl)alanine)-CYEK-(L-citrulline)-PYR-(L-citrulline)-CR, covalently linked to a phospholipid, was used for targeting a lipid-based gene delivery vehicle to CXCR4⁺-cells. Characterization of transfection activity was done *in vitro* using a transformed rat glioma cell line (RG2) that expresses CXCR4. The substitution of the targeting lipid at increasing mole percentages in the place of helper lipids yielded a progressive increase in reporter gene expression, reaching a maximum of 2.5 times the control value at 20 mol% of ligand. The substitution of helper lipids with cysteine-derivatized phospholipid analog or phosphatidylethanolamine resulted in a progressive decrease in transfection activity, with complete inactivation of the complex occurring at 20 mol%. A DNA dose-response with 10 mol% of lipopeptide reduced the effective DNA dose at least five-fold with regard to the number of transfected cells and >20-fold with regard to the amount of gene expression. Gene transfer to rat endothelial cells was studied in the context of an arterial organ culture. Mesenteric arteries were cannulated and maintained in culture for up to 4 days. CXCR4 cell-surface expression on endothelial cells was induced after overnight incubation with vascular endothelial growth factor (VEGF). Gene transfer studies showed that only the peptide-targeted lipoplexes transfected the endothelium, and only after CXCR4 had been induced with VEGF. These results demonstrate that non-viral transfection complexes can be targeted to cells expressing CXCR4, and that gene transfer is dependent upon cell surface receptor expression levels.

Received 7 June 2006; accepted 15 September 2007; advance online publication 15 January 2008. doi:10.1038/sj.mt.6300388

INTRODUCTION

A targeted non-viral gene delivery vehicle consists of plasmid DNA, formulated with either cationic lipids or polymers to which a ligand is attached. The ligand can be a protein, a peptide,

a carbohydrate, or a small-molecular-weight molecule that binds to receptors uniquely expressed on the target cell. This approach becomes particularly applicable in the treatment of cancer, wherein restriction of gene delivery to the tumor endothelium or tumor cells allows for expression of potent cytotoxic transgenes.

Systemic administration of cationic lipid/plasmid transfection complexes (lipoplexes) provides the greatest access to distant, vascularized tumors. However, lipoplexes also distribute to non-tumor tissue, with the highest expression usually observed in the lung endothelium¹⁻³ and the highest percentage of the injected dose being found in the liver and spleen.^{4,5} In mice bearing subcutaneous tumors, the level of gene expression in the tumors is two orders of magnitude lower than the expression in the lungs.^{3,6} One way to reduce the effect of gene transfer to non-cancerous tissue is to express a gene that selectively affects tumors, e.g., interleukin-12 (ref. 6) or p53.⁷ This approach restricts the number of candidate proteins for effective cancer gene therapy. In both viral and non-viral gene therapy, the development of gene delivery systems that shift the biodistribution away from the non-tumor bearing tissue and toward the tumors is actively being pursued.⁸⁻¹⁰ One way to shift both uptake and translation of exogenous DNA from non-tumor bearing tissues to tumor tissue is to actively target delivery vehicles by incorporating a ligand that binds to a surface-receptor on the tumor endothelium and/or tumor-cells. Non-viral gene delivery vehicles (*i.e.*, lipoplexes and polyplexes) are of interest in this attempt to achieve ligand-mediated tissue-specific delivery, because the efficiency and specificity of gene transfer can be enhanced by incorporating targeting ligands on the surface by means of minor modifications to the manufacturing process. Furthermore, these gene delivery vehicles show low immunogenicity and are relatively easy to produce on a large scale in comparison with viral vectors.^{11,12} The most successful approach has been to target the blood-brain barrier endothelium through the transferrin receptor, using either the natural ligand, transferrin, or an antibody to the receptor.¹³ One problem observed with this strategy of targeting the transferrin receptor is the ubiquitous expression of the receptor; e.g., gene transfer to the

*Current address: Vicat Incorporated, San Diego, California, USA.

Correspondence: Sean M. Sullivan, Vicat Incorporated, 10390 Pacific Center Court, San Diego, California 92121-4340, USA.
E-mail: ssullivan@vicat.com

blood-brain barrier endothelial cells also leads to hepatocyte targeting. Also, the use of large proteins such as monoclonal antibodies complicates the manufacturing process because of the heterogeneity of cross-linking chemistry, and stability issues regarding retention of native protein conformations. Stability issues are partly addressed by using small-molecular-weight ligands such as carbohydrates for hepatocyte targeting through asialoglycoprotein receptors,^{14,15} and RGD-peptides for tumor endothelial cell targeting through $\alpha_v\beta_3$ -integrin receptors.¹⁶⁻¹⁹ These examples clearly show the promise of ligand-targeted tissue-specific gene delivery, but the issues relating to identifying ligands that have sufficiently high affinity for their targets ($K_d \sim 1-10$ nmol/l), and identifying cell surface receptors that are either unique or display increased surface density on the targeted tissue, still remain a challenge. The goal of this study is to develop a peptide-targeted lipid-based gene delivery system for specific targeting of the tumor vasculature for treating brain cancer. The targeting strategy takes advantage of the fact that the endothelial cells of the vasculature are readily available to the lipoplexes. It is envisioned that further selectivity in gene transfer can be achieved by administration of the lipoplexes through a catheter downstream of the vascular bed of the tumor. The transfected endothelial cells will serve as producers of the gene product, which will affect both the tumor endothelium and the tumor cells.

This study was undertaken to characterize the gene transfer properties of a peptide-targeted lipoplex to proliferating endothelium through the CXCR4 chemokine receptor. This integral membrane protein is a seven-transmembrane G protein-coupled receptor for α -chemokines, and is the only receptor for stromal-derived factor 1- α (SDF1- α or CXCL12). This receptor is known to be expressed on a variety of solid tumors and on the endothelial cells of angiogenic vessels.²⁰⁻²² By incorporating a peptide ligand with high specificity for the receptor (4-fluorobenzoyl-RR-Nal-CY-Cit-KEPYR-Cit-CR; K_d of the original peptide is ~ 1.5 nmol/l²³) into liposomes, a CXCR4-targeted lipoplex is developed. Rat glioma cells (RG2s) expressing the receptor were successfully transfected with these targeted complexes, whereas complexes with control lipids were rendered inactive. With treatment using untargeted complexes, $\sim 40\%$ of the treated cells were found to be green fluorescent protein (GFP)-positive; the same efficiency can be achieved with a fivefold lower dose using targeted complexes. The targeted complexes were found to bind specifically to human umbilical vein endothelial cells (HUVECs) and endothelial cells of mesenteric arteries, but only after CXCR4 surface expression was induced by vascular endothelial growth factor (VEGF). More importantly, endothelial cells of a three-dimensional blood vessel organ culture have been shown to be successfully transfected with GFP, efficiently and specifically.

RESULTS

Transfection with CXCR4-ligand targeted lipoplexes leads to increased transfection-efficiency *in vitro*

The strategy for incorporating the targeting ligand into lipoplexes is to derivatize the CXCR4-binding peptide (4-fluorobenzoyl-RR-Nal-CY-Cit-KEPYR-Cit-CR; $K_d \sim 1.5$ nmol/l;²³) to a phospholipid (18:1 MPB PE) followed by incorporation of the lipopeptide into

the transfection complex. This was accomplished by reacting the peptide with *N*-Succinimidyl-S-acetylthioacetate (SATA), resulting in the modification of lysine at position 7 with a protected sulfhydryl group. The sulfhydryl was deprotected, and it reacted with the maleimide moiety attached to phosphatidylethanolamine (MPB-DOPE) creating a lipopeptide targeting ligand. The expression of CXCR4 on rat glioma cells (RG2) was verified by fluorescence-activated cell sorting (data not shown). CXCR4 surface-expression is not unique to RG2 cells, and many different types of tumor cells express this chemokine receptor.²⁶ The enhancement of transfection efficiency with the use of targeted lipoplexes was tested by formulating complexes with increasing amounts of targeting lipopeptide (0, 1, 5, 10, and 20 mol% of total lipid) into a cationic lipid mixture composed of 1-(*N*4-spermine)-2,3-dilaurylglycerol carbamate:lyso-phosphatidylcholine:glycerol monooleate:oleic acid (10:13:51:26 mol/mol). This formulation was selected because it forms micelles that can accommodate the lipopeptide before or after forming a complex with plasmid DNA. RG2 cells were transfected with lipoplexes containing DNA coding for firefly luciferase at a dose of 1 μ g plasmid DNA per 100,000 cells. Luciferase activity was measured 48 hours later. The results are shown in Figure 1. Luciferase expression levels of untargeted complexes were set at 100%, typically 10^4 relative light units, equivalent to 35 ng recombinant luciferase per well. One mole percent of lipopeptide increased the expression by 40% as compared to untargeted transfection complexes. This effect was enhanced by increasing the amounts of lipopeptide, leading to a twofold increase in luciferase activity as compared to the untargeted transfection complex. Titration of either MPB-DOPE derivatized with cysteine or DOPE alone produced the exactly opposite effect. The lipoplex produced decreasing luciferase expression with increasing amounts of the control lipids. One mole percent mol% of either of these lipids completely inactivated the transfection complex.

In order to further characterize the transfection-efficiency, CXCR4-lipopeptide was incorporated at 10 mol% of total lipid

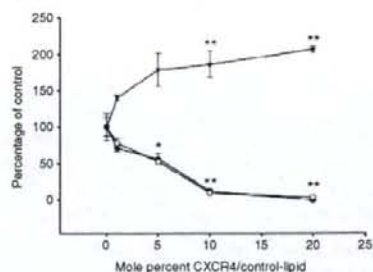


Figure 1 Increased efficiency of gene transfer of peptide targeted lipoplexes to rat glioma cells. Lipoplexes containing a firefly luciferase expression plasmid and increasing amounts of lipopeptide were used for transfecting RG2 cells [(DNA) = 1 μ g per well]. Luciferase activity was assayed after 48 hours. Control lipids 1,2-dioleoyl-*sn*-glycero-3-phosphoethanolamine (DOPE) and DOPE-MPB-Cys were titrated at the same mole percentage as the CXCR4 binding lipopeptide. The values shown are mean values \pm SD of at least three experiments. ** $P < 0.01$, * $P < 0.05$, as compared to control formulation (Student's *t*-test). Closed inverted triangles, CXCR4-lipopeptide; closed circles, DOPE-MPB-Cys; open circles, DOPE, MPB, *N*-[4-(*p*-maleimidophenyl)butylamide].

into the lipoplexes, and RG2 cells were transfected with GFP and luciferase with increasing dosages of plasmid DNA (0.1; 0.2; 0.5, and 1 $\mu\text{g}/100,000$ cells). At the lowest dose of 0.1 μg plasmid DNA/100,000 cells, ~20% of the cells were GFP-positive after transfection with the targeted lipoplex. At the highest dose of 1 μg DNA, >60% of the cells were GFP-positive when transfected with the targeted complex. Transfection with untargeted complexes yielded 10% GFP-positive cells at a dose of 0.5 μg DNA and 40% at 1 μg . Below 0.5 μg no GFP-positive cells were detected (Figure 2). In order to measure expression quantitatively and to determine whether lipoplexes are stable in the presence of serum, cells were transfected with targeted (10 mol% CXCR4-targeting lipid) and untargeted lipoplexes encoding for luciferase in the same DNA-dose range in serum-free or complete media. At the highest dose of 1 μg DNA the difference between targeted and untargeted lipoplexes was >25-fold both in the presence and absence of serum. Also, the transfection activity of the reagent is even higher in the presence of serum than in serum-free media (Figure 3).

These data show that the addition of the lipopeptide-targeting ligand to the lipoplex significantly increases the efficiency of gene transfer to the rat glioma cells expressing CXCR4. Second, the control lipid conditions indicated that unless the cells express

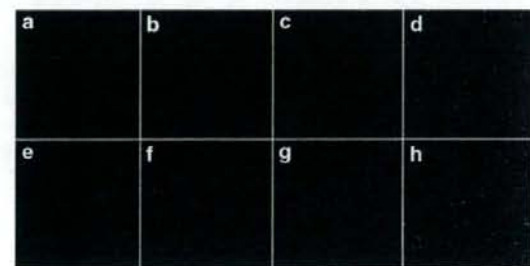


Figure 2 Green fluorescent protein (GFP) transfection of rat glioma cells with CXCR4-targeted and untargeted lipoplexes. CXCR4-lipopeptide was incorporated at 10 mol% into the lipoplexes encoding for GFP, and incubated with RG2. (a-d) Untargeted complexes and (e-h) CXCR4-targeted complexes. (a, e) 0.1 μg DNA/100,000 cells, (b, f) 0.2 μg , (c, g) 0.5 μg and (d, h) 1 μg . Original magnifications: $\times 40$.

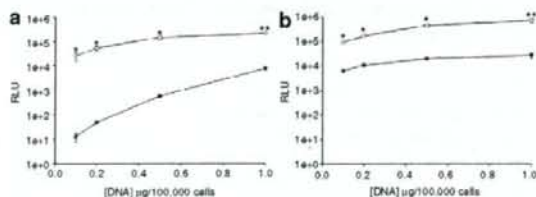


Figure 3 Luciferase transfection of rat glioma cells with CXCR4-targeted and untargeted lipoplexes. CXCR4-lipopeptide was incorporated at 10 mol% into the lipoplexes encoding for luciferase, and incubated with RG2 cells (a) in the absence of and (b) in the presence of 10% fetal bovine serum. Luciferase activity was assayed after 48 hours. The values shown are mean values \pm SD of at least three experiments. ** $P < 0.01$, * $P < 0.05$, as compared to untargeted formulation at the same dose (Student's *t*-test). Closed circles, untargeted; open circles, CXCR4-lipopeptide targeted. RLU, relative light unit.

the appropriate receptor, transfection is reduced at low mole percentages and completely inhibited at a higher mole percentage of control lipid.

CXCR4-expression on HUVEC is induced by VEGF-A

The overall goal of the research is to develop a ligand-targeted lipoplex specifically directed to tumor vasculature for the purpose of treating brain tumors. Success will depend upon the plasma membrane surface density of CXCR4 on tumor endothelial cells. HUVECs were substituted for the RG2 cells. Flow cytometry showed that the mean geometric log mean fluorescence intensity (MFI, arbitrary units) \pm SEM value ($n = 3$) for CXCR4 is 55.9 ± 52.51 , a value three to fivefold lower than the corresponding value for $\alpha_5\beta_1$ -integrin-receptor, basic fibroblast growth factor-receptor, and two isoforms of the VEGF-receptor (Flk1 and Flt1). Incubation with 50 ng/ml recombinant VEGF-A for 24 hours increases the MFI for CXCR4 to 248.27 ± 34.31 , a value comparable to the MFI of the other receptors measured. We did not find that VEGF has a significant influence on the surface expression of any of the other receptors tested (Figure 4). A time- and concentration-course was conducted, and the induction of CXCR4 in response to VEGF was found to plateau after ~16 hours. The increase in MFI for CXCR4 was the same for VEGF-concentrations in the range from 20 to 100 ng/ml (data not shown).

Specific binding of CXCR4-targeted liposomes to VEGF-stimulated HUVEC

The specific binding of the lipopeptide to CXCR4 on the surface of HUVECs was tested in the context of a multivalent display platform. The lipopeptide was incorporated at 20 mol% into unilamellar liposomes composed of 1,2-dioleoyl-*sn*-glycero-3-phosphocholine/Chol which were fluorescently labeled with 5 mol% of NBD-DOPE (~100 nm). The liposomes were incubated for 1 hour with HUVECs, with and without VEGF-induced CXCR4, at increasing doses (1, 3, 10, and 30 $\mu\text{mol/l}$ lipid). After 1 hour at 37 $^{\circ}\text{C}$, the cells were lysed and analyzed for total cell-associated fluorescence. Endothelial cells that had not been treated with VEGF were found to bind CXCR4-targeted liposomes to the

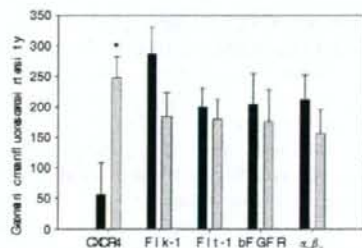


Figure 4 The effect of vascular endothelial growth factor-A (VEGF-A) on the surface expression of several receptors on human umbilical vein endothelial cells (HUVECs). HUVECs were incubated with 50 ng/ml recombinant rat VEGF-A for 24 hours, after which the surface expression of the indicated receptors was determined by flow cytometry. A total of 10,000 events were measured, and the geometric log mean fluorescence intensity \pm SEM is depicted as a graph. * $P < 0.05$ (Student's *t*-test). bFGFR, basic fibroblast growth factor receptor.